

Figure 4. Dendritic cells from oral-cavity-draining cervical lymph nodes induce Foxp3⁺ T-regs. (A) CLNs were stained with Foxp3 (red), CD4 (green) and CD11c (blue). Representative of three similar separate experiments. (B) OT II CD4⁺ T cells (5×10^4) were cultured with dendritic cells (DCs) from CLN, ALN, or MLN (5×10^4) with or without OVA peptide. After 5 days, cells were stained with Foxp3, CD25 and CD4. The plots were gated on CD4⁺ T cells. Representative of four separate experiments. (C) As in (A), but the graphic shows a summary of four separate experiments. P value provided is by paired t-test. "n.s."="not significant". doi:10.1371/journal.pone.0051665.g004

Furthermore, we found that DCs from oral-cavity-draining CLNs induce Foxp3⁺T-regs in the presence of antigen, as do DCs from MLNs (Fig.4B). It has been reported that cutaneous CD103⁺DCs induce Foxp3⁺T-regs using RALDH2, as intestinal CD103⁺DCs do [47]. Here, we would like to propose that DCs in the oral cavity use a different mechanism(s) to induce Foxp3⁺Tregs from DCs in the intestine. First, CLNs have few CD103⁺ DCs

compared with MLNs (Fig. 5B). Second, DCs from CLNs do not express RALDH2 at the mRNA level (Fig. 5A). We have not yet found any specific DC subset in the oral-cavity-draining CLNs. However, CD8⁻ classical DCs are increased in CLNs versus ALNs. Our previous report showed that CD8⁺DEC205⁺DCs induce Foxp3⁺T-regs from Foxp3⁻ cells and that CD8⁻33D1⁺DCs expand natural occurring Foxp3⁺T-regs

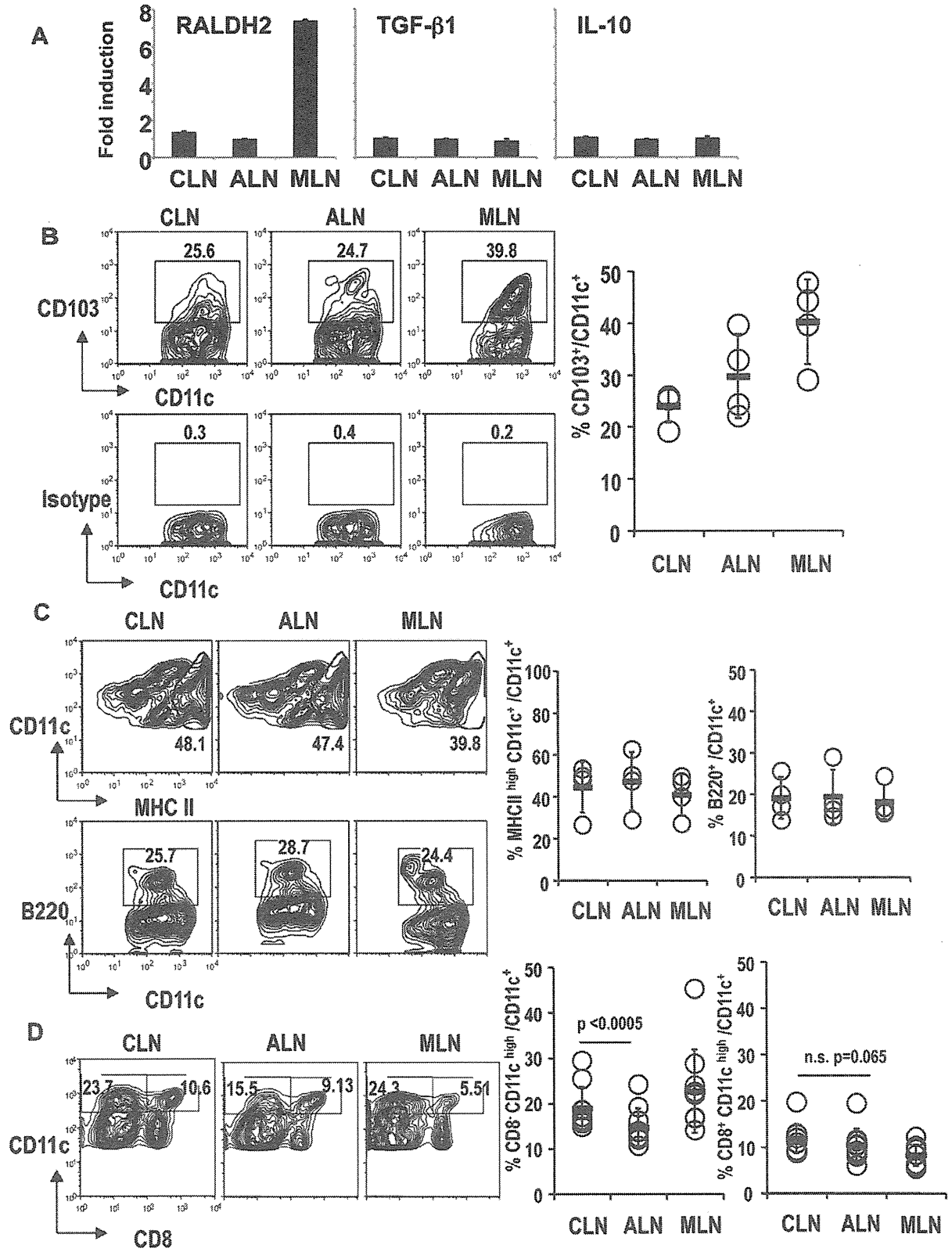


Figure 5. Phenotype of dendritic cells from cervical lymph nodes. (A) DCs from CLN, ALN, and MLN were freshly prepared from B6 mice. mRNA was prepared and real-time PCR was performed. Expression of each sample was normalized to GAPDH mRNA expression and fold increase of each sample was calculated relative to the expression at 0 h. One of two separate experiments is shown. (B) DCs from CLN, ALN, and MLN were analyzed for the expression of CD103. The plots were gated on CD11c⁺ cells. The isotype control for CD103 is shown at the bottom. The graphic shows a summary of four separate experiments. Average \pm SD is shown. (C) As in (B), DCs from CLN, ALN, and MLN were analyzed for the expression of MHC class II or B220. The plots were gated on CD11c⁺ cells. The graphic shows a summary of four separate experiments. Average \pm SD is shown. (D) As in (B), DCs from CLN, ALN, and MLN were analyzed for the expression of CD8. The plots were gated on CD11c⁺ cells. The graphic shows a summary of 10 separate experiments. P value provided is by paired t-test. "n.s." = "not significant". doi:10.1371/journal.pone.0051665.g005

[6,11]. Thus, it seems possible that CD8⁻DCs in CLNs may participate in expanding natural occurring Foxp3⁺T-regs.

Recently, it has been reported that recently activated Foxp3⁺T-regs from CLNs accumulated in CLNs after adoptive transfer [48]. It was suggested that TCR-mediated signals upon antigen stimulation may play a key role in the site-specific accumulation of Foxp3⁺T-regs in CLNs. Taken together, oral-cavity-draining CLNs may be a special location where Foxp3⁺T-regs are induced and also accumulate.

Here we showed that Foxp3⁺T-regs are induced in oral-cavity-draining CLNs in a Myd88/TICAM1 independent manner and that DCs from oral-cavity-draining CLNs have the capacity to induce Foxp3⁺Tregs on antigen stimulation. The mechanisms by which DCs to induce Foxp3⁺T-regs may differ from those in the intestine. We propose that Foxp3⁺T-regs play an important role in maintaining tolerance in the oral cavity to suppress Th17, as in the intestine. DCs from CLNs play a key role in maintaining tolerance upon oral antigen stimulation in the oral cavity. Further studies are required to identify the mechanism(s) by which DCs to induce Foxp3⁺T-regs in the oral cavity.

Materials and Methods

Mice

C57BL6J (B6) mice were from Japan Clea (Tokyo). Myd88 KO mice were from Dr. Shizuo Akira (Osaka University). TICAM-1 KO mice were established in our laboratory [29,30]. OT-II OVA CD4 T cell receptor transgenic mice were kindly provided by Dr. Kazuya Iwabuchi (Kitasato University). The mice were maintained in the Hokkaido University Animal Facility in a specific pathogen-free condition. All experiments used mice between 6-12-week-old mice at the time of first procedure. All mice were used according to the guidelines of the institutional animal care and use committee of the Hokkaido University, who approved this study (ID number: 08-0243, "Analysis of immune modulation by toll-like receptors.").

Antibodies and Reagents

PE-conjugated CD103, CD25 (PC61), Alexa-488 conjugated anti-CD25 (7D4), FITC, biotin or APC conjugated CD4 (RM4-5), CD11c, B220, NK1.1, purified anti-CD16/CD32 (2.4G2) antibodies were from Biogenex (San Diego, CA). Anti-CD11c, and streptavidin microbeads were from Miltenyi Biotec (Gladbach, Germany). CFSE was from Molecular Probes (Eugene, OR). PE conjugated anti-mouse ROR- γ t antibody and the anti-mouse Foxp3 (FJK-16s) staining kit were from eBioscience (San Diego, CA). LPS free OVA protein was from Seikagaku Co.(Tokyo, Japan).

Cell Isolation

CD4⁺ T cells were first negatively separated by MACS beads from lymph nodes and spleen cell suspensions (>90%; Miltenyi Biotec). CD4⁺ T cells were sometimes further purified by FACS Aria II (BD Bioscience, Franklin Lakes, NJ). CD11c⁺ DCs from

spleen, CLNs, ALNs, or MLNs were selected with anti-CD11c beads (Miltenyi Biotec) [7,10].

Co-culture with T cells and DCs

CD4⁺T cells from OT II transgenic mice were cultured with DCs at 0 or 0.01- μ M OVA peptide for 5 days. After 5 days, each culture was stained with Foxp3, following the manufacturer's protocol. Cells were acquired by FACS calibur flow cytometer (BD). Analyses were performed using the Flowjo software (TreeStar, USA).

Adoptive Transfer of OT-II CD4⁺ T cells

CD4⁺T cells from OT II transgenic mice were labeled with 5 μ M CFSE, and 1×10^6 T cells were injected intravenously into B6 recipients. One day later, OVA protein was administered sublingually. After 3 days, mice were sacrificed, and CLNs and ALNs were stained with CD4 and CFSE dilution was investigated. Cells were assessed by FACS calibur (BD). Analyses were performed using the Flowjo software (TreeStar, USA).

Quantitative PCR

Total RNA was isolated with TRIzol (Invitrogen), and reverse-transcribed with the High Capacity cDNA Transcription Kit (ABI) according to manufacturer's instructions. qPCR was performed with the Step One Real-Time PCR system (ABI). All primers for real-time PCR have been reported previously [27,28].

Measuring Cytokine Production

The purified DCs (1×10^5) were cultured in serum free RPMI medium for 20 h. The concentrations of TGF- β in the supernatants were measured by TGF-BELISA kit (R&D). Following the manufacturer's instructions, we measured the TGF- β with or without activation of the latent form of TGF- β . Culture supernatants with OT II CD4⁺T cells and DCs were measured for IL-10 by ELISA (eBiosciences) or Cytometric Bead Array (BD Bioscience). Analysis with the Cytometric Bead Array was performed according to the manufacturer's instructions.

Confocal Microscopy

CLNs were sectioned, fixed with acetone, and stained with anti-CD4-FITC and CD11c-APC antibodies. After permeabilization with the buffer from the Foxp3 staining kit (eBioscience), they were stained with an anti-Foxp3-PE antibody. They were washed and observed by confocal microscopy (LSM510 META, Zeiss, Jena, Germany).

Supporting Information

Figure S1 CD25⁺ and CD25⁻ Foxp3⁺ T-regs in lymph nodes and spleen. (A) CLN, ALN, ILN, MLN and Sp from B6 mice were analyzed for the expression of Foxp3 and CD25. The isotype control for Foxp3 is shown at the bottom. Plots were gated on CD4⁺ T cells. Representative of 2 separate experiments is

shown. (B) As in (A), but the frequency of CD25⁺ or CD25⁻ Foxp3⁺ T-regs/CD4⁺T cells were shown. (TIF)

Figure S2 The frequency of CD11c⁺ DC is similar between CLN and ALN. (A) CLN or ALN from one B6 mouse were digested by collagenase and stained with anti-CD11c and CD8 Abs. Representative of 5 separate experiments is shown. (B) The frequency of CD11c⁺ cells/total LN cells in one mouse is shown. A summary of 5 separate experiments. P value provided is by paired t-test. "n.s." = "not significant". (TIF)

References

- Sakaguchi S, Yamaguchi T, Nomura T, Ono M (2008) Regulatory T cells and immune tolerance. *Cell* 133: 775–787.
- Sakaguchi S, Miyara M, Costantino CM, Hafler DA (2010) FOXP3⁺ regulatory T cells in the human immune system. *Nature reviews Immunology* 10: 490–500.
- Rudenski AY (2011) Regulatory T cells and Foxp3. *Immunological reviews* 241: 260–268.
- Bour-Jordan H, Bluestone JA (2009) Regulating the regulators: costimulatory signals control the homeostasis and function of regulatory T cells. *Immunological reviews* 229: 41–66.
- Yamazaki S, Inaba K, Tarbell KV, Steinman RM (2006) Dendritic cells expand antigen-specific Foxp3⁺ CD25⁺ CD4⁺ regulatory T cells including suppressors of alloreactivity. *Immunological reviews* 212: 314–329.
- Yamazaki S, Steinman RM (2009) Dendritic cells as controllers of antigen-specific Foxp3⁺ regulatory T cells. *Journal of dermatological science* 54: 69–75.
- Yamazaki S, Iyoda T, Tarbell K, Olson K, Velinzon K, et al. (2003) Direct expansion of functional CD25⁺ CD4⁺ regulatory T cells by antigen-processing dendritic cells. *The Journal of experimental medicine* 198: 235–247.
- Fehervari Z, Sakaguchi S (2004) Control of Foxp3⁺ CD25⁺CD4⁺ regulatory cell activation and function by dendritic cells. *International immunology* 16: 1769–1780.
- Yamazaki S, Patel M, Harper A, Bonito A, Fukuyama H, et al. (2006) Effective expansion of alloantigen-specific Foxp3⁺ CD25⁺ CD4⁺ regulatory T cells by dendritic cells during the mixed leukocyte reaction. *Proceedings of the National Academy of Sciences of the United States of America* 103: 2758–2763.
- Yamazaki S, Bonito AJ, Spisek R, Dhodapkar M, Inaba K, et al. (2007) Dendritic cells are specialized accessory cells along with TGF- β for the differentiation of Foxp3⁺ CD4⁺ regulatory T cells from peripheral Foxp3 precursors. *Blood* 110: 4293–4302.
- Yamazaki S, Dudziak D, Heidkamp GF, Fiorese C, Bonito AJ, et al. (2008) CD8⁺ CD205⁺ splenic dendritic cells are specialized to induce Foxp3⁺ regulatory T cells. *Journal of immunology* 181: 6923–6933.
- Darrasse-Jeze G, Deroubaix S, Mouquet H, Victora GD, Eisenreich T, et al. (2009) Feedback control of regulatory T cell homeostasis by dendritic cells in vivo. *The Journal of experimental medicine* 206: 1853–1862.
- Izcue A, Coombes JL, Powrie F (2009) Regulatory lymphocytes and intestinal inflammation. *Annual review of immunology* 27: 313–338.
- Barnes MJ, Powrie F (2009) Regulatory T cells reinforce intestinal homeostasis. *Immunity* 31: 401–411.
- Hand T, Belkaid Y (2010) Microbial control of regulatory and effector T cell responses in the gut. *Current opinion in immunology* 22: 63–72.
- Coombes JL, Siddiqui KR, Arancibia-Carcamo CV, Hall J, Sun CM, et al. (2007) A functionally specialized population of mucosal CD103⁺ DCs induces Foxp3⁺ regulatory T cells via a TGF- β and retinoic acid-dependent mechanism. *The Journal of experimental medicine* 204: 1757–1764.
- Sun CM, Hall JA, Blank RB, Bouladoux N, Oukka M, et al. (2007) Small intestine lamina propria dendritic cells promote de novo generation of Foxp3⁺ T reg cells via retinoic acid. *The Journal of experimental medicine* 204: 1775–1785.
- Manicassamy S, Reizis B, Ravindran R, Nakaya H, Salazar-Gonzalez RM, et al. (2010) Activation of beta-catenin in dendritic cells regulates immunity versus tolerance in the intestine. *Science* 329: 849–853.
- Atarashi K, Tanoue T, Shima T, Imaoka A, Kuwahara T, et al. (2011) Induction of colonic regulatory T cells by indigenous Clostridium species. *Science* 331: 337–341.
- Round JL, Lee SM, Li J, Tran G, Jabri B, et al. (2011) The Toll-like receptor 2 pathway establishes colonization by a commensal of the human microbiota. *Science* 332: 974–977.
- Huber S, Gagliani N, Esplugues E, O'Connor W Jr, Huber FJ, et al. (2011) Th17 cells express interleukin-10 receptor and are controlled by Foxp3- and Foxp3⁺ regulatory CD4⁺ T cells in an interleukin-10-dependent manner. *Immunity* 34: 554–565.
- Chaudhry A, Samstein RM, Treuting P, Liang Y, Pils MC, et al. (2011) Interleukin-10 signaling in regulatory T cells is required for suppression of Th17 cell-mediated inflammation. *Immunity* 34: 566–578.
- Avila M, Ojcius DM, Yilmaz O (2009) The oral microbiota: living with a permanent guest. *DNA and cell biology* 28: 405–411.
- Sansonetti PJ (2011) To be or not to be a pathogen: that is the mucosally relevant question. *Mucosal immunology* 4: 8–14.
- Grice EA, Kong HH, Conlan S, Deming CB, Davis J, et al. (2009) Topographical and temporal diversity of the human skin microbiome. *Science* 324: 1190–1192.
- Costello EK, Lauber CL, Hamady M, Fierer N, Gordon JL, et al. (2009) Bacterial community variation in human body habitats across space and time. *Science* 326: 1694–1697.
- Manicassamy S, Ravindran R, Deng J, Oluoch H, Denning TL, et al. (2009) Toll-like receptor 2-dependent induction of vitamin A-metabolizing enzymes in dendritic cells promotes T regulatory responses and inhibits autoimmunity. *Nature medicine* 15: 401–409.
- Yamazaki S, Okada K, Maruyama A, Matsumoto M, Yagita H, et al. (2011) TLR2-dependent induction of IL-10 and Foxp3⁺CD25⁺CD4⁺ regulatory T cells prevents effective anti-tumor immunity induced by Pam2 lipopeptides in vivo. *PLoS One* 6: e18833.
- Oshiumi H, Matsumoto M, Funami K, Akazawa T, Seya T (2003) TICAM-1, an adaptor molecule that participates in Toll-like receptor 3-mediated interferon-beta induction. *Nature immunology* 4: 161–167.
- Akazawa T, Ebihara T, Okuno M, Okuda Y, Shingai M, et al. (2007) Antitumor NK activation induced by the Toll-like receptor 3-TICAM-1 (TRIF) pathway in myeloid dendritic cells. *Proceedings of the National Academy of Sciences of the United States of America* 104: 252–257.
- Mucida D, Park Y, Kim G, Turovskaya O, Scott I, et al. (2007) Reciprocal TH17 and regulatory T cell differentiation mediated by retinoic acid. *Science* 317: 256–260.
- Ivanov II, McKenzie BS, Zhou L, Tadokoro CE, Lepelley A, et al. (2006) The orphan nuclear receptor ROR γ directs the differentiation program of proinflammatory IL-17⁺ T helper cells. *Cell* 126: 1121–1133.
- Onodera T, Jang MH, Guo Z, Yamasaki M, Hirata T, et al. (2009) Constitutive expression of IDO by dendritic cells of mesenteric lymph nodes: functional involvement of the CTLA-4/B7 and CCL22/CCR4 interactions. *Journal of immunology* 183: 5608–5614.
- Ochando JC, Homma C, Yang Y, Hidalgo A, Garin A, et al. (2006) Alloantigen-presenting plasmacytoid dendritic cells mediate tolerance to vascularized grafts. *Nature immunology* 7: 652–662.
- Hanabuchi S, Ito T, Park WR, Watanabe N, Shaw JL, et al. (2010) Thymic stromal lymphopoietin-activated plasmacytoid dendritic cells induce the generation of FOXP3⁺ regulatory T cells in human thymus. *Journal of immunology* 184: 2999–3007.
- Chen W, Liang X, Peterson AJ, Munn DH, Blazar BR (2008) The indoleamine 2,3-dioxygenase pathway is essential for human plasmacytoid dendritic cell-induced adaptive T regulatory cell generation. *Journal of immunology* 181: 5396–5404.
- Seneschal J, Clark RA, Gehad A, Baecher-Allan CM, Kupper TS (2012) Human epidermal Langerhans cells maintain immune homeostasis in skin by activating skin resident regulatory T cells. *Immunity* 36: 873–884.
- Azukizawa H, Dohler A, Kanazawa N, Nayak A, Lipp M, et al. (2011) Steady state migratory R α B⁺ langerin⁺ dermal dendritic cells mediate peripheral induction of antigen-specific CD4⁺ CD25⁺ Foxp3⁺ regulatory T cells. *European journal of immunology* 41: 1420–1434.
- Kautz-Neu K, Noordegraaf M, Dinges S, Bennett CL, John D, et al. (2011) Langerhans cells are negative regulators of the anti-Leishmania response. *The Journal of experimental medicine* 208: 885–891.
- Gomez de Agüero M, Vocanson M, Hacini-Rachinel F, Taillardet M, Sparwasser T, et al. (2012) Langerhans cells protect from allergic contact dermatitis in mice by tolerizing CD8⁺ T cells and activating Foxp3⁺ regulatory T cells. *The Journal of clinical investigation* 122: 1700–1711.
- Sutmoller RP, den Brok MH, Kramer M, Bennis EJ, Toonen LW, et al. (2006) Toll-like receptor 2 controls expansion and function of regulatory T cells. *The Journal of clinical investigation* 116: 485–494.
- Round JL, Mazmanian SK (2010) Inducible Foxp3⁺ regulatory T-cell development by a commensal bacterium of the intestinal microbiota. *Proceedings of the National Academy of Sciences of the United States of America* 107: 12204–12209.

Acknowledgments

We thank Dr. Kazuya Iwabuchi and Dr. Shizuo Akira for the mice. We appreciate Dr. Ralph M. Steinman (Rockefeller University) for his encouragement and visiting our lab. We thank for Ms. Akiko Nishioka and Ms. Saori Kasuya for their technical assistance.

Author Contributions

Conceived and designed the experiments: SY. Performed the experiments: A. Maruyama SY KO. Analyzed the data: SY A. Maruyama MM A. Morita TS. Wrote the paper: SY.

43. Naik S, Bouladoux N, Wilhelm C, Molloy MJ, Salcedo R, et al. (2012) Compartmentalized Control of Skin Immunity by Resident Commensals. *Science*.
44. Zhang X, Gao L, Lei L, Zhong Y, Dube P, et al. (2009) A MyD88-dependent early IL-17 production protects mice against airway infection with the obligate intracellular pathogen *Chlamydia muridarum*. *Journal of immunology* 183: 1291–1300.
45. Atarashi K, Nishimura J, Shima T, Umesaki Y, Yamamoto M, et al. (2008) ATP drives lamina propria T(H)17 cell differentiation. *Nature* 455: 808–812.
46. Ivanov II, Atarashi K, Manel N, Brodie EL, Shima T, et al. (2009) Induction of intestinal Th17 cells by segmented filamentous bacteria. *Cell* 139: 485–498.
47. Guillemins M, Crozat K, Henri S, Tamoutounour S, Grenot P, et al. (2010) Skin-draining lymph nodes contain dermis-derived CD103⁺ dendritic cells that constitutively produce retinoic acid and induce Foxp3⁺ regulatory T cells. *Blood* 115: 1958–1968.
48. Lieberman SM, Kim JS, Corbo-Rodgers E, Kambayashi T, Maltzman JS, et al. (2012) Site-specific accumulation of recently activated CD4⁺ Foxp3⁺ regulatory T cells following adoptive transfer. *European journal of immunology* 42: 1429–1435.

Toll-like receptor 3 signaling converts tumor-supporting myeloid cells to tumoricidal effectors

Hiroaki Shime^a, Misako Matsumoto^a, Hiroyuki Oshiumi^a, Shinya Tanaka^b, Akio Nakane^c, Yoichiro Iwakura^d, Hideaki Tahara^e, Norimitsu Inoue^f, and Tsukasa Seya^{a,1}

^aDepartment of Microbiology and Immunology, and ^bDepartment of Cancer Pathology, Graduate School of Medicine, Hokkaido University, Kita-ku, Sapporo 060-8638, Japan; ^cDepartment of Microbiology and Immunology, Graduate School of Medicine, Hirosaki University, Zaifu-cho, Hirosaki 036-8562, Japan; ^dLaboratory of Molecular Pathogenesis, Center for Experimental Medicine and Systems Biology, and ^eDepartment of Surgery and Bioengineering, Advanced Clinical Research Center, Institute of Medical Science, University of Tokyo, Shirokanedai, Minato-ku, Tokyo 108-8639, Japan; and ^fDepartment of Molecular Genetics, Osaka Medical Center for Cancer, Nakamichi, Higashinari-ku, Osaka 537-8511, Japan

Edited by Ruslan Medzhitov, Yale University School of Medicine, New Haven, CT, and approved December 20, 2011 (received for review August 11, 2011)

Smoldering inflammation often increases the risk of progression for malignant tumors and simultaneously matures myeloid dendritic cells (mDCs) for cell-mediated immunity. PolyI:C, a dsRNA analog, is reported to induce inflammation and potent antitumor immune responses via the Toll-like receptor 3/Toll-IL-1 receptor domain-containing adaptor molecule 1 (TICAM-1) and melanoma differentiation-associated protein 5/IFN- β promoter stimulator 1 (IPS-1) pathways in mDCs to drive activation of natural killer cells and cytotoxic T lymphocytes. Here, we found that i.p. or s.c. injection of polyI:C to Lewis lung carcinoma tumor-implant mice resulted in tumor regression by converting tumor-supporting macrophages (Mfs) to tumor suppressors. F4/80⁺/Gr1⁻ Mfs infiltrating the tumor respond to polyI:C to rapidly produce inflammatory cytokines and thereafter accelerate M1 polarization. TNF- α was increased within 1 h in both tumor and serum upon polyI:C injection into tumor-bearing mice, followed by tumor hemorrhagic necrosis and growth suppression. These tumor responses were abolished in TNF- α ^{-/-} mice. Furthermore, F4/80⁺ Mfs in tumors extracted from polyI:C-injected mice sustained Lewis lung carcinoma cytotoxic activity, and this activity was partly abrogated by anti-TNF- α Ab. Genes for supporting M1 polarization were subsequently up-regulated in the tumor-infiltrating Mfs. These responses were completely abrogated in TICAM-1^{-/-} mice, and unaffected in myeloid differentiation factor 88^{-/-} and IPS-1^{-/-} mice. Thus, the TICAM-1 pathway is not only important to mature mDCs for cross-priming and natural killer cell activation in the induction of tumor immunity, but also critically engaged in tumor suppression by converting tumor-supporting Mfs to those with tumoricidal properties.

Toll-like receptor | tumor-associated macrophages | TRIF

Inflammation followed by bacterial and viral infections triggers a high risk of cancer and promotes tumor development and progression (1, 2). Long-term use of anti-inflammatory drugs has been shown to reduce—if not eliminate—the risk of cancer, as demonstrated by a clinical study of aspirin and colorectal cancer occurrence (3). Inflammatory cytokines facilitate tumor progression and metastasis in most cases. Innate immune response and the following cellular events are closely concerned with the formation of the tumor microenvironment (4, 5).

By contrast, inflammation induced by microbial preparations was applied to patients with cancer for therapeutic potential as Coley vaccine with some success. A viral replication product, dsRNA and its analog polyI:C (6, 7), induced acute inflammation, and has been expected to be a promising therapeutic agent against cancer. Although polyI:C exerts life-threatening cytopenia (8), trials for its clinical use as an adjuvant continued because of its high therapeutic potential (9, 10). Pathogen-associated molecular patterns (PAMPs) and host cell factors induced secondary to PAMP–host cell interaction act as a double-edged sword in cancer prognosis and require understanding their multifarious functional properties in the tumor environment.

Recent advances in the study of innate immunity show how polyI:C suppresses tumor progression (11). PolyI:C is a synthetic

compound that serves as an agonist for pattern-recognition receptors (PRRs), Toll-like receptor 3 (TLR3), and melanoma differentiation-associated protein 5 (MDA5) (12–14). Although TLR3 and MDA5 signals are characterized as myeloid differentiation factor 88 (MyD88) independent (15, 16), they have immune effector-inducing properties (12–14, 17). TLR3 couples with the Toll-IL-1 receptor domain-containing adaptor molecule 1 (TICAM-1, also known as TRIF), and MDA5 couples with the IFN- β promoter stimulator 1 (IPS-1, also known as Cardif, MAVS, or VISA) (11, 15). Possible functions for the TICAM-1 and IPS-1 signaling pathways have been investigated by using gene-disrupted mice (15); although they activate the same downstream transcription factors NF- κ B and IFN regulatory factor 3 (IRF-3) (15, 18), they appear to distinctly modulate myeloid dendritic cells (mDCs) and macrophages (Mfs) to drive effector lymphocytes (19, 20).

Tumor microenvironments frequently involve myeloid-derived suppressor cells (MDSCs), tumor-associated macrophages (TAMs), and immature mDCs (1, 21). These myeloid cells express PRR through which they are functionally activated. Once the inflammation process is triggered, immature mDCs turn mature so that they are capable of antigen cross-presentation and able to activate immune effector cells, which would act to protect the host system and damage the undesirable tumor cells (22). However, TAMs and MDSCs play a major role in establishing a favorable environment for tumor cell development by suppressing antitumor immunity and recruiting host immune cells to support tumor cell survival, motility, and invasion (23–25). Although these myeloid cell scenarios have been studied with interest, how the PRR signal in these myeloid cells links regulation of tumor progression has yet to be elucidated.

Here we show that TICAM-1 but not IPS-1 signal in tumor-infiltrating Mfs is engaged in conversion of the TAM-like Mfs to tumoricidal effectors. We investigated the molecular mechanisms in Mfs underlying the phenotype switch from tumor supporting to tumor suppressing by treating cells with polyI:C and found that the TICAM-1–inducing TNF- α and M1 polarization are crucial for eliciting tumoricidal activity in TAMs.

Results

In Vivo Effect of PolyI:C on Implant Lewis Lung Carcinoma Tumor. I.p. injection of polyI:C rapidly induced hemorrhagic necrosis in 3LL tumors implanted in WT mice, which was established >12 h after polyI:C treatment (Fig. 1A). The polyI:C-dependent hemorrhagic necrosis did not occur in TNF- α ^{-/-} mice (Fig. 1A). Histological

Author contributions: H.S., M.M., and T.S. designed research; H.S., H.O., and S.T. performed research; H.O., A.N., Y.I., and H.T. contributed new reagents/analytic tools; M.M. and N.I. analyzed data; and H.S. and T.S. wrote the paper.

The authors declare no conflict of interest.

This article is a PNAS Direct Submission.

¹To whom correspondence should be addressed. E-mail: seya-tu@pop.med.hokudai.ac.jp.

This article contains supporting information online at www.pnas.org/lookup/suppl/doi:10.1073/pnas.1113099109/-DCSupplemental.

and immunohistochemical analysis revealed vascular damage in the necrotic lesion, where disruption of vascular endothelial cells was indicated by fragmented CD31⁺ marker (Fig. S1). Although the polyI:C signal is delivered by TICAM-1 and IPS-1 adaptors (11, 13), the hemorrhagic necrosis was largely alleviated in TICAM-1^{-/-} mice but not in IPS-1^{-/-} mice (Fig. 14). The results suggest that polyI:C is a reagent that induces Lewis lung carcinoma (3LL) hemorrhagic necrosis, and the TICAM-1 pathway and its products, including TNF- α , are preferentially involved in this response.

3LL implant tumors grew well in WT C57BL6 mice. PolyI:C, when i.p. injected, resulted in tumor growth retardation (Fig. 1B). The retardation of tumor growth by polyI:C was also impaired in TNF- α ^{-/-} mice (Fig. 1B), suggesting that TNF- α is a critical effector for not only induction of hemorrhagic necrosis but also further 3LL tumor regression. To investigate the signaling pathway involved in the tumor growth retardation by polyI:C, we challenged WT, MyD88^{-/-}, TICAM-1^{-/-}, and IPS-1^{-/-} mice with 3LL implantation and then treated the mice with i.p. injection of polyI:C. 3LL growth retardation was observed in both IPS-1^{-/-} (Fig. 1C) and MyD88^{-/-} mice, to a similar extent to WT mice. In contrast, polyI:C-dependent tumor growth retardation was abrogated in TICAM-1^{-/-} mice (Fig. 1D). The size differences of the implanted tumors became significant within 2 d after polyI:C treatment, suggesting that the molecular effector for tumor regression is induced early and its upstream is TICAM-1. Similar results were obtained with MC38 implant tumor (Fig. S24), which is TNF- α sensitive and MHC class I positive (Table S1) (26).

PolyI:C is a reagent that induces natural killer (NK) cell activation in MHC class I-negative tumors (12), and 3LL cells are class I negative and NK cell sensitive (Table S1) (27, 28). We tested whether NK cells activated by polyI:C damage the 3LL tumor in mice. Tumor growth was not affected by pretreatment of the mice with anti-NK1.1 Ab in this model (Fig. S3). Thus, NK cells, at least the NK1.1⁺ cells, have a negligible ability to retard tumor growth in vivo.

PolyI:C Induces TNF- α Through the TICAM-1 Pathway in Mice. To test whether polyI:C treatment had elicited TNF- α production in vivo, we investigated the cytokine profiles of serum from polyI:C-stimulated WT and IPS-1^{-/-} and TICAM-1^{-/-} mice by ELISA. Prominent differences in TNF- α levels were observed in serum collected from polyI:C-injected WT and TICAM-1^{-/-} mice. Serum TNF- α levels in WT and IPS-1^{-/-} mice were significantly higher than that in TICAM-1^{-/-} mice within 1 h after polyI:C injection (Fig. S4 A and B). IFN- β is a main output for polyI:C stimulation (11), and its production was decreased in TICAM-1^{-/-} mice and totally abrogated in IPS-1^{-/-} mice (Fig. S4C). Taken together, the data indicate that the TICAM-1 pathway was able to sustain a high TNF- α level in the early phase of polyI:C treatment, which is independent of IPS-1 and subsequent production of IFN- β .

TICAM-1⁺ Cells in Tumor Produces TNF- α in Response to PolyI:C Stimulation. Using the 3LL implant WT, IPS-1^{-/-}, and TICAM-1^{-/-} mouse models, we tested whether polyI:C-induced early TNF- α was responsible for the lately observed tumor regression. Time-course analyses of the polyI:C-induced TNF- α protein levels were performed by ELISA using serum samples and tumors extracted from the experimental mice. The tumor TNF- α levels in WT and IPS-1^{-/-} mice increased at 2 h after polyI:C i.p. injection (Fig. 24). The serum TNF- α levels in both were rapidly up-regulated within 1 h after polyI:C injection, although in WT the levels continued to increase but in IPS-1^{-/-} mice gradually decreased (Fig. 2B). In TICAM-1^{-/-} mice, however, no appreciable up-regulation of TNF- α protein was detected in either tumor or serum samples during the early time-course tested. To test whether the induced TNF- α protein was generated de novo in tumors, we examined the corresponding mRNA levels in excised tumors (Fig. 2C and Table S2). The TNF- α mRNA levels peaked between 1 and 2 h after polyI:C injection, whereas the TNF- α protein level was kept high at >2 h after polyI:C injection

in tumor as well as serum. In the TICAM-1^{-/-} mice, TNF- α production was largely abrogated in the tumor and serum samples, suggesting that TNF- α was mainly produced and secreted in response to polyI:C stimulation from the TLR3/TICAM-1⁺ cells within the tumor.

F4/80⁺/Gr-1⁻ Mfs in 3LL Tumor Produce TNF- α Leading to Tumor Damage. We next investigated the cell types that had infiltrated the tumor by using various Mf markers in FACS analysis and tumor samples extracted at 1 h after polyI:C injection. We discovered that CD45⁺ cells in the tumor produced TNF- α in response to polyI:C (Fig. 34). The major population of those CD45⁺ cells was determined to be of CD11b⁺ myeloid-lineage cells that coexpressed F4/80⁺, Gr1⁺, or CD11c⁺. A small population of NK1.1⁺ cells was also detected. CD4⁺ T cells, CD8⁺ T cells, and B cells were rarely detected in these implant tumors (Fig. S54). Moreover, F4/80⁺/Gr-1⁻ cells were found to be the principal contributors to polyI:C-mediated TNF- α production (Fig. 3 B and C). F4/80⁺ cells in 3LL tumor highly expressed macrophage mannose receptor (MMR; CD206), a M2 macrophage marker, in contrast to splenic F4/80⁺CD11b⁺ cells. Both TNF- α -producing and -nonproducing F4/80⁺ cell populations in 3LL tumor showed indistinguishable levels of CD206 (Fig. S6), and dissimilar to MDSCs or splenic Mfs, as determined by the surface marker profiles (Table S3). Thus, the source of the TNF- α -producing cells in tumor is likely F4/80⁺ Mfs with a TAM-like feature.

We harvested F4/80⁺ cells from tumor samples extracted from WT and TICAM-1^{-/-} mice at 30 min after polyI:C injection. These cells were used in *in vitro* experiments to verify the TNF- α -producing abilities and 3LL cytotoxicity properties (Fig. 4 A and B). WT F4/80⁺ Mfs exhibited normal TNF- α -producing function and were able to kill 3LL cells upon exposure. This tumoricidal activity was ~50% neutralized by the addition of anti-TNF- α Ab (Fig. 4C), although incomplete inhibition by this mAb may reflect participation of other factors in TNF- α cytotoxicity. Furthermore, when active TNF- α protein (rTNF- α) was added exogenously to 3LL cell culture, the cytotoxic effects were still present and occurred in a dose-dependent manner (Fig. 4D). TNF- α -producing ability was also observed in F4/80⁺ cells from implant tumor of MC38, B16D8, or EL4, and only the MC38 tumor was remediable by TICAM-1-derived TNF- α (Fig. S2 B and C). The MC38 tumor contained the F4/80⁺/CD11b⁺/Gr1⁻ cells, as in the 3LL tumor (Fig. S5B).

IFN- β did not enhance rTNF- α -mediated 3LL killing efficacy (Fig. S7A), a finding that was consistent with previously published data (29). No effect of IRF3/7 on polyI:C-induced 3LL tumor regression in vivo was confirmed using IRF3/7 double-knockout mice. However, polyI:C-dependent tumor regression was abrogated in 3LL-bearing IFN- α / β receptor (IFNAR)^{-/-} mice (Fig. S7B). Quantitative PCR analysis of cells from WT vs. IFNAR^{-/-} tumor-bearing mice revealed that the TLR3 level was basally low and not up-regulated in response to polyI:C in tumor-infiltrating F4/80⁺ Mfs of IFNAR^{-/-} mice (Fig. S7C). Accordingly, the TNF- α level was not up-regulated in tumor and serum in polyI:C-stimulated IFNAR^{-/-} mice (Fig. S7D). Thus, basal induction of type I IFN serves as a critical factor for TLR3 function in tumor F4/80⁺ Mfs to produce TNF- α in vivo. These results suggest that the direct effector for 3LL cytotoxicity by polyI:C involves TNF- α , which is derived from TICAM-1 downstream independent of the IRF3/7 axis. Our results indicate that cytotoxic TNF- α is produced via a distinct route from initial type I IFN and downstream of TICAM-1 in F4/80⁺ TAM-like Mfs. Type I IFN do not synergistically act with TNF- α on 3LL killing, but is required to complete the TLR3/TICAM-1 pathway.

These results were confirmed by *in vitro* assay, wherein the F4/80⁺ Mfs harvested from 3LL tumors in WT, TICAM-1^{-/-}, IPS-1^{-/-}, and TLR3^{-/-} mice were stimulated with polyI:C (Fig. S84). Both TNF- α release and 3LL cytotoxic abilities of polyI:C-stimulated F4/80⁺ Mfs were specifically abrogated by the absence of TICAM-1 and TLR3 (Fig. S8 A and B). IPS-1 or

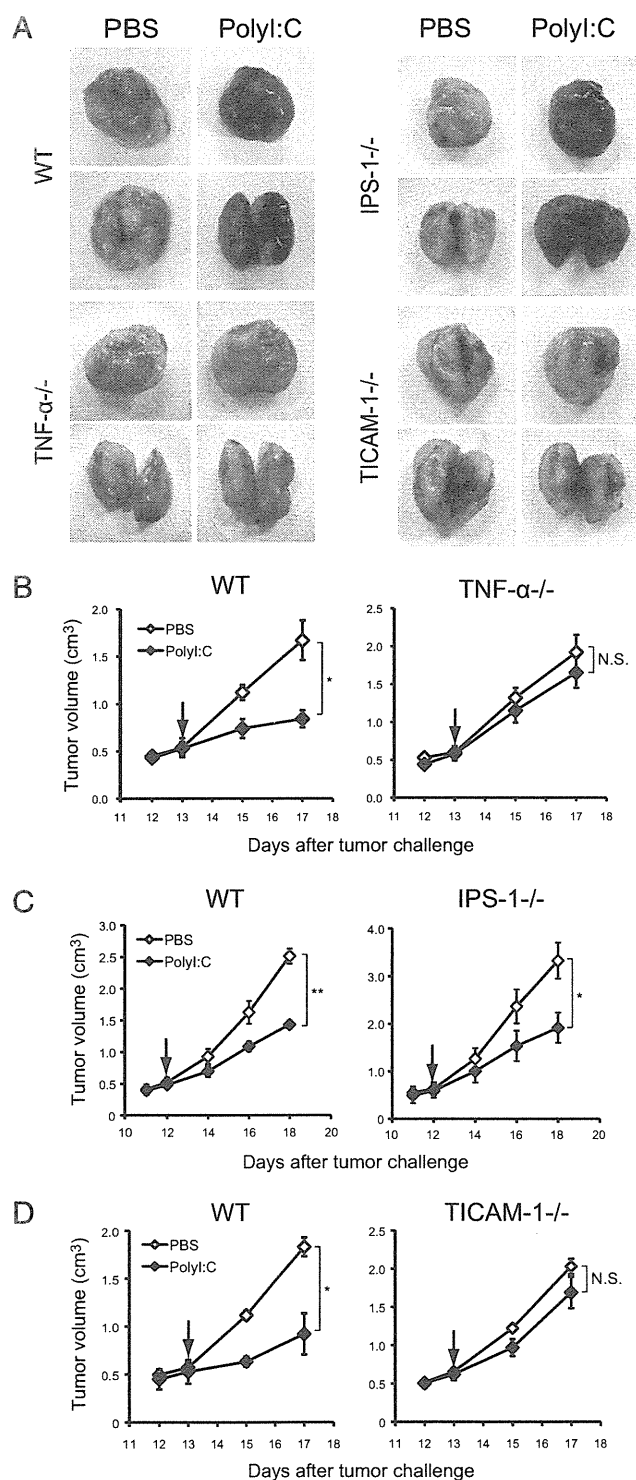


Fig. 1. Antitumor activity of polyI:C against 3LL tumor cells is mediated by the TICAM-1 pathway in vivo. (A) Representative photographs of 3LL tumors excised from WT, TNF- $\alpha^{-/-}$, TICAM-1 $^{-/-}$, and IPS-1 $^{-/-}$ mice. Whole tumor (Upper) and bisected tumor (Lower) are shown. (B–D) On day 0, 3LL tumor cells (3×10^6) were s.c. implanted into B6 WT (B–D), TNF- $\alpha^{-/-}$ (B), TICAM-1 $^{-/-}$ (C), and IPS-1 $^{-/-}$ (D) mice. PolyI:C i.p. injection was started on the day indicated by arrow, then repeated every 4 d. Data are shown as tumor average size \pm SE; $n = 3$ –4 mice per group. * $P < 0.05$; ** $P < 0.001$. N.S., not significant. A representative experiment of two with similar outcomes is shown.

MyD88 in F4/80 $^{+}$ Mfs had no or minimal effect on the TNF- α tumoricidal effect against 3LL tumors. PolyI:C did not directly exert a cytotoxic effect on 3LL tumor cells (Fig. S8C).

Role of the IPS-1 Pathway in F4/80 $^{+}$ Cells. Both TICAM-1 and IPS-1 are known to converge their signals on transcription factors NF- κ B and IRF-3, which drive expression of TNF- α and IFN- β , respectively. PolyI:C-induced TNF- α production was reduced in F4/80 $^{+}$ cells extracted from tumors of TICAM-1 $^{-/-}$ mice, but not in samples of IPS-1 $^{-/-}$ mice. We examined the expression of IFN- β in these cells after polyI:C stimulation. Compared with F4/80 $^{+}$ cells from WT mice, IFN- β expression and production was barely decreased in IPS-1 $^{-/-}$ F4/80 $^{+}$ cells, but largely impaired in TICAM-1 $^{-/-}$ F4/80 $^{+}$ cells (Fig. S9A) as other cytokines tested. M1 Mf-associated cytokines/chemokines were generally reduced in TICAM-1 $^{-/-}$ F4/80 $^{+}$ cells compared with WT and IPS-1 $^{-/-}$ cells >4 h after polyI:C stimulation (Fig. S9A), whereas M2 Mf-associated genes were barely affected by TICAM-1 disruption or polyI:C stimulation (Fig. S9B).

Most types of Mfs are known to express TLR3 in mice (30). Messages and proteins for type I IFN induction were conserved in the F4/80 $^{+}$ tumor-infiltrating Mfs (Fig. S10 A–C). However, the TLR3 mRNA level was low in macrophage colony-stimulating factor (M-CSF)-derived Mfs compared with TAMs (Fig. S10D). We further examined whether IFN- β production might also have relied on the TICAM-1 pathway in other types of Mfs upon stimulation with polyI:C. In contrast to the F4/80 $^{+}$ cells isolated from tumor (Fig. S11 A and B), the IPS-1 pathway was indispensable for polyI:C-mediated IFN- β production in mouse peritoneal Mfs and M-CSF-induced bone marrow-derived Mfs (Fig. S11 C and E). However, IPS-1 only slightly participated in polyI:C-mediated TNF- α production in these Mf subsets (Fig. S11 D and F). It appears then that the IPS-1 pathway is able to signal the presence of polyI:C and subsequently induce type I IFN. TICAM-1 is the protein that induces effective TNF- α in all subsets of Mfs.

PolyI:C Influences Polarization of TAMs. Plasticity is a characteristic feature of Mfs (25). Various factors and signals can influence polarization of Mf cells to induce the M1/M2 transition, which is accompanied by a substantial change in the Mf cell's expression profile of cytokines and chemokines. Previous studies have demonstrated that Mfs that have infiltrated into tumor are of the M2-polarized phenotype, which is known to contribute to tumor progression. To test the effects of polyI:C on the polarization of tumor-infiltrated Mf cells, we analyzed the gene expression profiles of these cells following in vitro polyI:C stimulation, and representative profiles were confirmed by quantitative PCR (Fig. 5 A and B). The mRNA expressions were increased for M1 Mf markers IL-12p40, IL-6, CXCL11, and IL-1 β at 4 h after in vitro polyI:C treatment, as were mRNA levels of TNF- α and ex vivo results. The M2 Mf markers arginase-1 (*Arg1*), chitinase 3-like 3 (*Chi3l3*), and MMR (*Mrc1*) were unchanged, compared with unstimulated levels; however, the M2 Mf marker IL-10, a regulatory cytokine, was induced. In addition, there was no difference observed in the mRNA expression levels of MMP9 (*Mmp9*) and VEGFA (*Vegfa*), both of which are involved in tissue remodeling and angiogenesis events of tumor progression (Fig. 5C). The polyI:C-induced M1 markers and IL-10 expression that were up-regulated in WT and IPS-1 $^{-/-}$ F4/80 $^{+}$ cells were found to be abrogated in TICAM-1 $^{-/-}$ F4/80 $^{+}$ cells (Fig. 5 A and B), reinforcing the results obtained with F4/80 $^{+}$ Mfs isolated from 3LL tumors in mice injected with polyI:C (Fig. S9 A and B). It appears that TICAM-1 is responsible for the M1 polarization of F4/80 $^{+}$ Mf cells in tumors, but has no effect on M2 markers. We further examined the expression of IRF-5 and IRF-4, which are considered the master regulators for M1 and M2 polarization, respectively (31, 32). As expected, polyI:C induced IRF-5 mRNA expression, but had no effect on IRF-4 mRNA expression in vitro (Fig. 5 A and B). Jmjd3, a histone H3K27 demethylase involved in IRF-4 expression, is reportedly induced by TLR stimulation (33). In our study, polyI:C stimulation increased Jmjd3 mRNA in F4/80 $^{+}$ cells

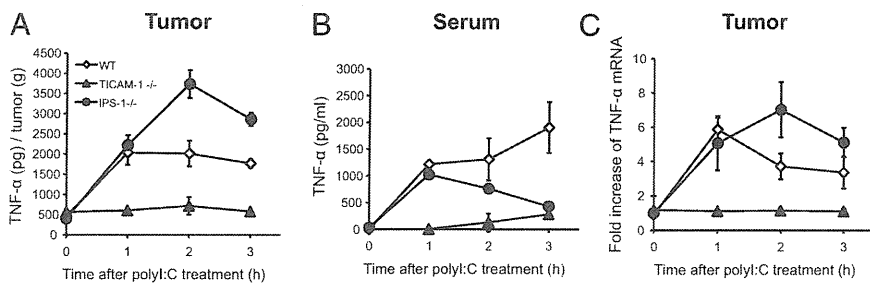


Fig. 2. TNF- α production in tumor and serum of polyI:C-injected 3LL tumor-bearing mice. Mice bearing 3LL tumor were i.p. injected with 200 μ g polyI:C. Tumor (A) and serum (B) were collected at 0, 1, 2, and 3 h after polyI:C injection, and TNF- α concentration was determined by ELISA. TNF- α level in tumor is presented as [TNF- α protein (pg)/tumor weight (g)]. (C) Tumors were isolated from polyI:C-injected tumor-bearing WT, TICAM-1^{-/-}, and IPS-1^{-/-} mice, and TNF- α mRNA was measured by quantitative PCR; $n = 3$. Data are shown as average \pm SD. A representative experiment of two with similar outcomes is shown.

(Fig. 5B). The polyI:C-triggered M1 gene expression continued long in tumor-infiltrated Mfs, a finding that may further explain the tumor-suppressing feature of these Mfs, in addition to the concern of early inducing TNF- α .

Discussion

In this study we demonstrated that the tumor-supporting properties of tumor-infiltrating F4/80⁺ Mfs characterized by M2 markers are dynamic and able to shift to an M1-dominant state upon the particular signal provided by PRRs. In 3LL tumors that express minimal amounts of MHC class I/II and recruit a large amount of myeloid cells, F4/80⁺ Mfs function to sustain the tumor in the surrounding microenvironment. This tumor-supporting environment can be disrupted by stimulation with an RNA duplex through a TICAM-1 signal and subsequent induction of mediators such as TNF- α . Thus, the TICAM-1 signal in tumor-infiltrating Mfs plays a key role in TNF- α and M1 shift-mediated tumor regression. These results were confirmed using another cell line, MC38 colon adenocarcinoma (34), although MC38 cells express MHC class I. B16D8 melanoma (12) and EL4 lymphoma (35) were resistant to TNF- α , but their F4/80⁺ Mfs still possessed TNF- α -inducing potential by stimulation with polyI:C; their susceptibilities to polyI:C reportedly depend on other effectors (12, 35). These results may partly explain the reported findings that tumors regressed in patients with simultaneous virus infection (36, 37), and that tumor growth was inhibited by polyI:C injection in tumor-bearing mice (6, 7).

In contrast, polyI:C-stimulated PEC or bone marrow-derived Mfs induce type I IFN via the IPS-1 pathway unlike the case of tumor-infiltrating F4/80⁺ Mfs. Nevertheless, all of these Mf

subsets produce proinflammatory cytokines, including TNF- α , in a TICAM-1-dependent manner. Thus, the key question that arose was why predominant TICAM-1 dependence for polyI:C-mediated production of TNF- α occurred in F4/80⁺ tumor-infiltrating Mfs leading to tumor regression. A marked finding is that the TLR3 protein level is high in tumor-infiltrating Mfs compared with other sources of Mfs (Fig. S10). In addition, the IPS-1 pathway is unresponsive to polyI:C if the polyI:C is exogenously added to the tumor-infiltrating Mfs without transfection reagents. The cytoplasmic dsRNA sensors normally work for IFN induction in tumor F4/80⁺ Mfs if the polyI:C is transfected into the cells. TICAM-1-dependent TNF- α production by F4/80⁺ Mfs (Fig. S11 D and F) occurs partly because F4/80⁺ Mfs express a high basal level of TLR3 and fail to take up extrinsic polyI:C into the cytoplasm. Of many subsets of Mfs, these properties (38) are unique to the F4/80⁺ Mfs.

Hemorrhagic necrosis and tumor size reduction are closely correlated with constitutive production of TNF- α (39, 40). The association of PRR-derived TNF- α and hemorrhagic necrosis of tumor has been described earlier. Carswell et al. (41) showed that TNF- α is robustly expressed in mouse serum following treatment with bacillus Calmette-Guérin and endotoxin. Bioassay of TNF- α as reflected by the degree of hemorrhagic necrosis of transplanted Meth A sarcoma in BALB/c mice led the authors to speculate that Mfs are responsible for TNF- α induction. Many years later, Dougherty et al. (42) identified the mechanism responsible for the TNF- α production associated with antitumor activity; macrophages isolated from tumors in mice with inactivating mutation in the TLR4 gene [Lps(d) in C3H/HeJ] expressed 5- to 10-fold less TNF- α than tumors in WT mice. This finding represents a unique recognition of a PRR contributing to the cancer phenotype. Subsequent studies determined that MyD88 is involved in the induction of TNF- α via TLR4 binding to its cognate ligand, lipid A endotoxin (15, 43). Because the TLR3 signal is independent of MyD88, this MyD88 concept is not applicable to the present study on polyI:C-dependent tumor regression.

Alternatively, endotoxin/lipid A may have activated TICAM-1 in previous reports on TLR4-derived TNF- α because TLR4 can recruit TICAM-1 in addition to MyD88 (15). The lipid A derivative monophospholipid A preferentially activates the TICAM-1 pathway of TLR4 (43). It is likely that TICAM-1 participates in TLR4-mediated tumor regression in addition to MyD88, although MyD88 is not involved in the polyI:C signaling. This point was further proven using TNF- α ^{-/-} mice: TICAM-1-derived TNF- α in F4/80⁺ Mf cells has a critical role in the induction of tumor necrosis and regression by polyI:C. The results are consistent with the finding that both TICAM-1 and IPS-1 pathways are able to induce NF- κ B activation secondary to polyI:C stimulation, and indeed their signals converge at the I κ B kinase complex (18).

TICAM-1 is able to induce many of the IFN-inducible genes that MyD88 cannot in mDCs (44). In both cases of TICAM-1 and MyD88 stimulation, tumor-infiltrating Mfs facilitate the expression of many genes in addition to TNF- α . The M2 phenotype of F4/80⁺ Mfs or tumor-associated Mfs is modified dependent on these additional factors. IFNAR facilitates polyI:C-mediated tumor regression in tumor-bearing mice, lack of which results in no induction of TLR3 (Fig. S7). Thus, preceding the polyI:C

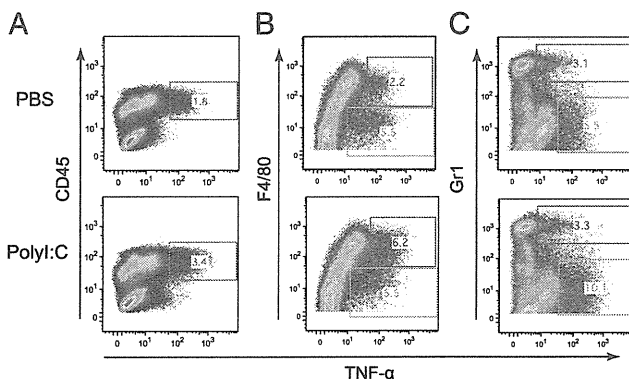


Fig. 3. F4/80⁺ cells are responsible for the polyI:C-induced elevation of TNF- α production in tumor. Mice bearing 3LL tumors were i.p. injected with 200 μ g polyI:C. TNF- α -producing cells in tumors of polyI:C- or PBS-injected mice were examined by immunohistochemical staining and flow cytometry to determine intracellular cytokine expression profiles of CD45⁺ cells (A), F4/80⁺ cells (B), and Gr1⁺ cells (C). CD45⁺ cells in tumor were gated and are shown in B and C. A representative experiment of two with similar outcomes is shown. TNF- α ⁺ gating squares are shown in red (positive) and green (negative).

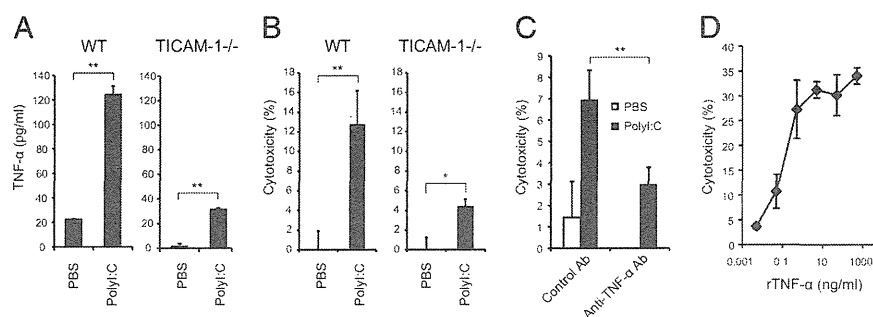


Fig. 4. PolyI:C enhances TNF- α production and cytotoxicity of F4/80 $^{+}$ cells in tumor. PolyI:C (200 μ g) or PBS was i.p. injected into 3LL tumor-bearing WT mice. After 30 min, F4/80 $^{+}$ cells isolated from tumor were cultured for 24 h and TNF- α concentration in the conditioned medium was determined by ELISA (A). In parallel, the cytotoxicity of tumor-infiltrating F4/80 $^{+}$ cells against 3LL tumor cells was measured by 51 Cr-release assay (B). Anti-TNF- α neutralization antibody or control antibody was added (10 μ g/mL) to mixed culture of isolated tumor-infiltrating F4/80 $^{+}$ cells and 3LL tumor cells (C). (D) Cytotoxic activity of TNF- α against 3LL tumor cells. Recombinant TNF- α was added to 51 Cr-labeled 3LL tumor cell culture at various concentrations. After 20 h, cytotoxicity was measured; $n = 3$. Data are shown as average \pm SD. * $P < 0.05$, ** $P < 0.001$. A representative experiment of three with similar outcomes is shown.

response, minute type I IFN of undefined source has to be provided to set the TLR3/TICAM-1 pathway, which may primarily fail in IFNAR $^{-/-}$ mice. Cellular effectors, cytotoxic T lymphocyte (CTL) and NK cells, are induced secondary to activation of IFN-inducible genes in a late phase of polyI:C-stimulated myeloid cells (45–47). The relationship among the TICAM-1-mediated type I IFN liberation, these late-phase effectors, and tumor regression remains an open question in this setting.

M1 Mf cells function to protect the host against tumors by producing large amounts of inflammatory cytokines and activating the immune response (48, 49). However, distinct types of M2 cells differentiate when monocytes are stimulated with IL-4 and IL-13 (M2a), immune complexes/TLR ligands (M2b), or IL-10 and glucocorticoids (M2c) (50). In our study, polyI:C stimulation led to incremental expression of the M1 Mf-related genes. In contrast, polyI:C stimulation was not associated with M2 polarization, except for IL-10. Other genes related to angiogenesis and extravasation were not affected by polyI:C treatment. Thus, polyI:C was able to induce the characteristic M1 conversion and, in turn, contribute to tumor regression. It is notable that TAM cells usually have defective and delayed NF- κ B activation in response to different proinflammatory signals,

such as expression of cytotoxic mediators NO, cytokines, TNF- α , and IL-12 (51–53). These observations are in apparent contrast with the function of other resident Mf species. This discrepancy may again reflect a dynamic change in the tumor microenvironment during tumor progression.

In line with our findings, virus infection has been observed to instigate tumor regression in patients with cancer (36, 54). Gene therapy for cancer patients using virus-derived vectors has proved effective in reducing tumors in clinic (36, 37). Administration of dsRNA elicits IFN induction, NK cell activation, and CTL proliferation for antitumor effectors in vivo (19, 55). This is a unique finding that tumor-infiltrating Mfs are a target of dsRNA and converted from tumor supporters to tumoricidal effectors. Hence, the antitumor effect of dsRNA adjuvant is ultimately based on the liberation of type I IFN, functional maturation of mDCs, and modulation of tumor-infiltrating Mfs, where TICAM-1 is a crucial transducer in eliciting antitumor immunity.

Methods

Inbred C57BL/6 WT mice were purchased from CLEA Japan, Inc. TICAM-1 $^{-/-}$ and IPS-1 $^{-/-}$ mice were generated in our laboratory and maintained as described previously. IRF-3/7 double-KO mice were a gift from T. Taniguchi

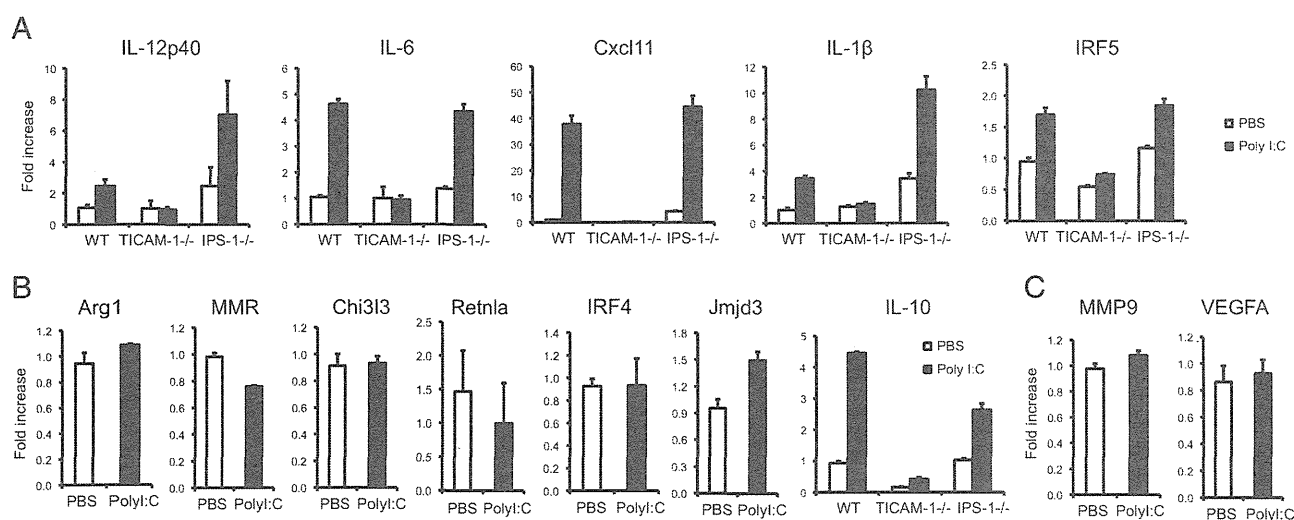


Fig. 5. PolyI:C induces M1 polarization of TAMs. F4/80 $^{+}$ cells were isolated from 3LL tumor and stimulated with polyI:C (50 μ g/mL) for 4 h. Total RNA was extracted and used to analyze the transcript expression levels of M1 (A) and M2 (B and C) markers; $n = 3$. Data are shown as average \pm SD. A representative experiment of two with similar outcomes is shown.

(University of Tokyo, Tokyo, Japan). TNF- $\alpha^{-/-}$ mice were kindly provided by A. Nakane (Hirosaki University, Aomori, Japan) and Y. Iwakura (University of Tokyo). Mice 6–10 wk of age were used in all experiments. 3LL lung cancer cells were cultured at 37 °C under 5% CO₂ in RPMI containing 10% FCS, penicillin, and streptomycin. This study was carried out in strict accordance with the recommendations in the Guide for the Care and Use of Laboratory Animals of the National Institutes of Health. The protocol was approved by the Committee on the Ethics of Animal Experiments in the Animal Safety Center, Hokkaido University, Japan. All mice were used according to the guidelines of the Institutional Animal Care and Use Committee of Hokkaido

University, who approved this study as no. 08-0290, "Analysis of Anti-Tumor Immune Response Induced by the Activation of Innate Immunity."

Other detailed methods are provided in *SI Methods*.

ACKNOWLEDGMENTS. We thank Dr. T. Taniguchi (University of Tokyo) and D. M. Segal (EIB/NCI, Bethesda, MD) for kindly providing us with IRF-3/7 double KO mice and mAb against mouse TLR3. This work was supported in part by Grants-in-Aid from the Ministry of Education, Science, and Culture (MEXT), "The Carcinogenic Spiral" a MEXT Grant-in-Project, and the Ministry of Health, Labor, and Welfare of Japan, the Takeda Foundation, the Akiyama Foundation, and the Waxman Foundation.

- Grivnenkov SI, Greten FR, Karin M (2010) Immunity, inflammation, and cancer. *Cell* 140:883–899.
- de Visser KE, Eichten A, Coussens LM (2006) Paradoxical roles of the immune system during cancer development. *Nat Rev Cancer* 6:24–37.
- Chan AT, Ogino S, Fuchs CS (2007) Aspirin and the risk of colorectal cancer in relation to the expression of COX-2. *N Engl J Med* 356:2131–2142.
- Rakoff-Nahoum S, Medzhitov R (2007) Regulation of spontaneous intestinal tumorigenesis through the adaptor protein MyD88. *Science* 317:124–127.
- Chen GY, Shaw MH, Redondo G, Núñez G (2008) The innate immune receptor Nod1 protects the intestine from inflammation-induced tumorigenesis. *Cancer Res* 68:10060–10067.
- Sarma PS, Shiu G, Neubauer RH, Baron S, Huebner RJ (1969) Virus-induced sarcoma of mice: Inhibition by a synthetic polyribonucleotide complex. *Proc Natl Acad Sci USA* 62:1046–1051.
- Levy HB, Law LW, Rabson AS (1969) Inhibition of tumor growth by polyinosinic-polycytidylic acid. *Proc Natl Acad Sci USA* 62:357–361.
- Absher M, Stinebring WR (1969) Toxic properties of a synthetic double-stranded RNA. Endotoxin-like properties of poly I. poly C, an interferon stimulator. *Nature* 223:715–717.
- Talmadge JE, et al. (1985) Immunomodulatory effects in mice of polyinosinic-polycytidylic acid complexed with poly-L-lysine and carboxymethylcellulose. *Cancer Res* 45:1058–1065.
- Longhi MP, et al. (2009) Dendritic cells require a systemic type I interferon response to mature and induce CD4⁺ Th1 immunity with poly IC as adjuvant. *J Exp Med* 206:1589–1602.
- Matsumoto M, Seya T (2008) TLR3: Interferon induction by double-stranded RNA including poly(I:C). *Adv Drug Deliv Rev* 60:805–812.
- Akazawa T, et al. (2007) Antitumor NK activation induced by the Toll-like receptor 3-TICAM-1 (TRIF) pathway in myeloid dendritic cells. *Proc Natl Acad Sci USA* 104:252–257.
- Miyake T, et al. (2009) Poly I:C-induced activation of NK cells by CD8 α^+ dendritic cells via the IPS-1 and TRIF-dependent pathways. *J Immunol* 183:2522–2528.
- McCartney S, et al. (2009) Distinct and complementary functions of MDA5 and TLR3 in poly(I:C)-mediated activation of mouse NK cells. *J Exp Med* 206:2967–2976.
- Oshiumi H, Matsumoto M, Funami K, Akazawa T, Seya T (2003) TICAM-1, an adaptor molecule that participates in Toll-like receptor 3-mediated interferon-beta induction. *Nat Immunol* 4:161–167.
- Yoneyama M, et al. (2005) Shared and unique functions of the DExD/H-box helicases RIG-I, MDA5, and LGP2 in antiviral innate immunity. *J Immunol* 175:2851–2858.
- Takeuchi O, Akira S (2010) Pattern recognition receptors and inflammation. *Cell* 140:805–820.
- Sasai M, et al. (2006) NAK-associated protein 1 participates in both the TLR3 and the cytoplasmic pathways in type I IFN induction. *J Immunol* 177:8676–8683.
- Seya T, Matsumoto M (2009) The extrinsic RNA-sensing pathway for adjuvant immunotherapy of cancer. *Cancer Immunol Immunother* 58:1175–1184.
- Iwasaki A, Medzhitov R (2010) Regulation of adaptive immunity by the innate immune system. *Science* 327:291–295.
- Condeelis J, Pollard JW (2006) Macrophages: Obligate partners for tumor cell migration, invasion, and metastasis. *Cell* 124:263–266.
- Schuler G, Schuler-Thurner B, Steinman RM (2003) The use of dendritic cells in cancer immunotherapy. *Curr Opin Immunol* 15:138–147.
- Murdoch C, Muthana M, Coffelt SB, Lewis CE (2008) The role of myeloid cells in the promotion of tumour angiogenesis. *Nat Rev Cancer* 8:618–631.
- Borrello MG, Degl'Innocenti D, Pierotti MA (2008) Inflammation and cancer: The oncogene-driven connection. *Cancer Lett* 267:262–270.
- Biswas SK, Mantovani A (2010) Macrophage plasticity and interaction with lymphocyte subsets: Cancer as a paradigm. *Nat Immunol* 11:889–896.
- Farma JM, et al. (2007) Direct evidence for rapid and selective induction of tumor neovascular permeability by tumor necrosis factor and a novel derivative, colloidal gold bound tumor necrosis factor. *Int J Cancer* 120:2474–2480.
- Masuda H, et al. (2002) High levels of RAE-1 isoforms on mouse tumor cell lines assessed by the anti-pan-Rae-1 polyclonal antibody confers tumor cell cytotoxicity on mouse NK cells. *Biochem Biophys Res Commun* 290:140–145.
- Smyth MJ, et al. (2004) NKG2D recognition and perforin effector function mediate effective cytokine immunotherapy of cancer. *J Exp Med* 200:1325–1335.
- Remels L, Franssen L, Huygen K, De Baetselier P (1990) Poly I:C activated macrophages are tumoricidal for TNF- α -resistant 3LL tumor cells. *J Immunol* 144:4477–4486.
- Jelinek I, et al. (2011) TLR3-specific double-stranded RNA oligonucleotide adjuvants induce dendritic cell cross-presentation, CTL responses, and antiviral protection. *J Immunol* 186:2422–2429.
- Krausgruber T, et al. (2011) IRF5 promotes inflammatory macrophage polarization and TH1-TH17 responses. *Nat Immunol* 12:231–238.
- Satoh T, et al. (2010) The *Jmjd3-Irf4* axis regulates M2 macrophage polarization and host responses against helminth infection. *Nat Immunol* 11:936–944.
- De Santa F, et al. (2007) The histone H3 lysine-27 demethylase *Jmjd3* links inflammation to inhibition of polycomb-mediated gene silencing. *Cell* 130:1083–1094.
- Zitvogel L, et al. (1995) Cancer immunotherapy of established tumors with IL-12. Effective delivery by genetically engineered fibroblasts. *J Immunol* 155:1393–1403.
- Abe R, Peng T, Sailors J, Bucala R, Metz CN (2001) Regulation of the CTL response by macrophage migration inhibitory factor. *J Immunol* 166:747–753.
- Russell SJ (2002) RNA viruses as virotherapy agents. *Cancer Gene Ther* 9:961–966.
- Aghi M, Martuza RL (2005) Oncolytic viral therapies—the clinical experience. *Oncogene* 24:7802–7816.
- Watanabe A, et al. (2011) Raftlin is involved in the nucleocapture complex to induce poly(I:C)-mediated TLR3 activation. *J Biol Chem* 286:10702–10711.
- Mocellin S, Rossi CR, Pilati P, Nitti D (2005) Tumor necrosis factor, cancer and anti-cancer therapy. *Cytokine Growth Factor Rev* 16:35–53.
- Balkwill F (2009) Tumour necrosis factor and cancer. *Nat Rev Cancer* 9:361–371.
- Carswell EA, et al. (1975) An endotoxin-induced serum factor that causes necrosis of tumors. *Proc Natl Acad Sci USA* 72:3666–3670.
- Dougherty ST, Eaves CJ, McBride WH, Dougherty GJ (1997) Molecular mechanisms regulating TNF-alpha production by tumor-associated macrophages. *Cancer Lett* 111:27–37.
- Mata-Haro V, et al. (2007) The vaccine adjuvant monophosphoryl lipid A as a TRIF-biased agonist of TLR4. *Science* 316:1628–1632.
- Ebihara T, et al. (2010) Identification of a poly(I:C)-inducible membrane protein that participates in dendritic cell-mediated natural killer cell activation. *J Exp Med* 207:2675–2687.
- Akazawa T, et al. (2004) Adjuvant-mediated tumor regression and tumor-specific cytotoxic response are impaired in MyD88-deficient mice. *Cancer Res* 64:757–764.
- Akazawa T, et al. (2007) Tumor immunotherapy using bone marrow-derived dendritic cells overexpressing Toll-like receptor adaptors. *FEBS Lett* 581:3334–3340.
- Schulz O, et al. (2005) Toll-like receptor 3 promotes cross-priming to virus-infected cells. *Nature* 433:887–892.
- Mantovani A, Sica A, Locati M (2007) New vistas on macrophage differentiation and activation. *Eur J Immunol* 37:14–16.
- Martinez FO, Helming L, Gordon S (2009) Alternative activation of macrophages: An immunologic functional perspective. *Annu Rev Immunol* 27:451–483.
- Mantovani A, et al. (2004) The chemokine system in diverse forms of macrophage activation and polarization. *Trends Immunol* 25:677–686.
- Sica A, et al. (2000) Autocrine production of IL-10 mediates defective IL-12 production and NF-kappa B activation in tumor-associated macrophages. *J Immunol* 164:762–767.
- Torroella-Kouri M, et al. (2005) Diminished expression of transcription factors nuclear factor kappaB and CCAAT/enhancer binding protein underlies a novel tumor evasion mechanism affecting macrophages of mammary tumor-bearing mice. *Cancer Res* 65:10578–10584.
- Biswas SK, et al. (2006) A distinct and unique transcriptional program expressed by tumor-associated macrophages (defective NF-kappaB and enhanced IRF-3/STAT1 activation). *Blood* 107:2112–2122.
- Bluming AZ, Ziegler JL (1971) Regression of Burkitt's lymphoma in association with measles infection. *Lancet* 2:105–106.
- Matsumoto M, Oshiumi H, Seya T (2011) Antiviral responses induced by the TLR3 pathway. *Rev Med Virol* 21:67–77.

Supporting Information

Shime et al. 10.1073/pnas.1113099109

SI Methods

Reagents. PolyI:C was purchased from GE Healthcare, which was free from LPS contamination. TNF- α and IFN- β ELISA kit was purchased from eBioscience and PBL InterferonSource, respectively. Recombinant TNF- α was purchased from R&D Systems.

Tumor Cells and Tumor-Infiltrated Immune Cells. We first tested the amounts of macrophages (Mfs) in implant tumors formed in B6 mice. Mouse lymphoma (EL4), Lewis lung carcinoma (3LL), adenocarcinoma MC38, and melanoma (B16D8) lines grew well in the back of mice, and the Mf content was maximal in the 3LL tumor. MC38, a murine colon adenocarcinoma cell line, was a gift from S. A. Rosenberg (National Cancer Institute, Bethesda) (1). Hemorrhagic necrosis shown in Fig. 1A was typically induced in response to polyI:C in 3LL tumor. We then used the 3LL line for this study.

3LL cells were found to express very low amounts of detectable MHC class I or class II (Table S1), suggesting this cell type as a possible target for natural killer (NK) cells but not cytotoxic T lymphocytes (CTLs). 3LL cells were found to express appreciable amounts of the NKG2D ligand, retinoic acid-inducible gene 1, consistent with previous reports (Table S1) (2, 3). 3LL cells also expressed mRNA transcripts for Toll-like receptor 3 (TLR3), Toll-IL-1 receptor domain-containing adaptor molecule 1 (TICAM-1), IFN- β promoter stimulator 1 (IPS-1), and melanoma differentiation-associated protein 5 (MDA5). Exposure to polyI:C-stimulated peritoneal Mfs caused significant death of 3LL cells, which was likely an effect of liberated inflammatory cytokines such as TNF- α (4). Consistent with previously reported data about 3LL properties in vitro, the 3LL cells we used were not damaged by direct polyI:C treatment or exposure to 3LL-derived cytokines (Fig. S8C). When 3LL cells were implanted s.c. in mice, the resulting tumors were found to contain a high amount (>30%) of CD45.2⁺ cells (Fig. S5A). The major population of those CD45.2⁺ cells was determined to be of CD11b⁺ myeloid lineage cells that coexpressed F4/80⁺, Gr1⁺, or CD11c⁺. A small population of NK1.1⁺ cells was also detected. CD4⁺ T cells, CD8⁺ T cells, and B cells were rarely detected in these implant tumors (Fig. S5A).

Cytotoxic Activity Assay. Mice bearing 3LL tumor were injected i.p. with polyI:C. Mice were killed and F4/80⁺ cells were isolated from tumor by using MACS-positive selection beads (Miltenyi) as described previously. 3LL cells were labeled with ⁵¹Cr for 3–5 h and then washed three times with the medium. F4/80⁺ cells, and 3LL cells were cocultured at the indicated ratio. After 20 h, supernatants were harvested and ⁵¹Cr release was measured in each sample. Specific lysis was calculated by the following formula: cytotoxicity (%) = [(experimental release – spontaneous release) / (max release – spontaneous release)] \times 100.

Flow Cytometric Analysis. Mononuclear cells prepared from spleen and tumor were treated with anti-CD16/32 (no. 93) and stained with APC-anti-CD45.2 (no. 104), FITC-anti-CD11b (M1/70), PE-anti-GR1 (RB6-8C5), FITC-anti-CD11c (N418), PE- or APC-anti-F4/80 (BM8), PE-anti-NK1.1 (PK136), PE-anti-CD49b (DX5), PE-anti-CD3e (145-2C11), FITC-anti-CD4 (GK1.5), FITC-anti-CD8a (53-6.7), and PE- and anti-CD19 (MB19-1; eBioscience and Biolegend; Table S2). Samples were

analyzed with FACSCalibur (BD Biosciences), and data analysis was performed using FlowJo software (Tree Star). For intracellular cytokine staining, we freshly isolated tumors from polyI:C or PBS-injected mice at 1 h and incubated the cells in the presence of 10 μ g/mL Brefeldin A for 3 h. Cells were fixed and stained with the combination of anti-CD45.2 Ab and anti-F4/80 Ab or anti-Gr1 Ab, followed by permeabilizing and staining with anti-TNF Ab using BD Cytotfix/Cytoperm Kit (BD Biosciences).

Quantitative PCR Analysis. Tumor samples were cut into small pieces and homogenized with TRIzol Reagent (Invitrogen). Total RNA was isolated according to the manufacturer's instruction. Reverse transcription was performed using High-Capacity cDNA Reverse Transcription Kit (Applied Biosystems). Real-time PCR was performed with Power SYBR Green PCR Master Mix (Applied Biosystems) with a StepOne Real-Time PCR System (Applied Biosystems). Expression of the cytokine gene was normalized to the expression of *GAPDH*. We used primer pairs listed in Table S3. Data were analyzed by the $\Delta\Delta$ Ct method.

ELISA and Cytokine Beads Assay. Tumor samples were cut into small pieces and homogenized with CellLytic MT Mammalian Tissue Lysis/Extraction Reagent (Sigma) supplemented with Complete Protease Inhibitor Mixture (Roche) on ice. Lysate was centrifuged to remove insoluble materials, and the supernatant was used for ELISA. Serum cytokine concentration was determined by ELISA or cytokine bead assays. Data were shown as TNF- α (pg) per weight of tumor (g).

Histochemistry and Immunohistochemistry. 3LL tumor was fixed with buffered 10% formalin overnight and embedded in paraffin wax, and sections 4 μ m in thickness were stained with H&E. For immunohistochemistry, tumor was embedded in optimal cutting-temperature compound, and snap-frozen in liquid nitrogen. Cryosections 6 μ m in thickness were air-dried for 60 min and fixed for 15 min with prechilled acetone and then incubated with FITC-anti-CD31 antibody (390; BioLegend). The sections were mounted in Prolong Gold Antifade Reagent with DAPI (Invitrogen). Images were obtained with a Leica LSM510 confocal laser-scanning microscope.

Tumor Challenge and PolyI:C Treatment. Mice were shaved at the back and injected s.c. with 200 μ L of 3×10^6 3LL cells in PBS(-). Tumor size was measured using a caliper. Tumor volume was calculated using the following formula: tumor volume (cm³) = (long diameter) \times (short diameter)² \times 0.4. PolyI:C (250 μ g/head) with no detectable LPS was injected i.p. as indicated. In some cases, polymixin B-treated polyI:C was used. When an average tumor volume of 0.5–0.8 cm³ was reached, the treatment was started and repeated every 4 d.

Isolation of F4/80⁺ Cells from Tumor. Tumors formed by 3LL cells were excised at 2 wk after transplantation and treated with 0.05 mg/mL Collagenase I (Sigma), 0.05 mg/mL Collagenase IV (Sigma), 0.025 mg/mL hyaluronidase (Sigma), and 0.01 mg/mL DNase I (Roche) in HBSS at 37 $^{\circ}$ C for 10 min. F4/80⁺ cells were isolated by using biotinylated anti-F4/80 antibody (BM8) and Streptavidin MicroBeads (Miltenyi). We routinely prepared F4/80⁺ cells at >90% purity from tumor.

1. Zitvogel L, et al. (1995) Cancer immunotherapy of established tumors with IL-12. Effective delivery by genetically engineered fibroblasts. *J Immunol* 155:1393–1403.
2. Masuda H, et al. (2002) High levels of RAE-1 isoforms on mouse tumor cell lines assessed by the anti-pan-Rae-1 polyclonal antibody confers tumor cell cytotoxicity on mouse NK cells. *Biochem Biophys Res Commun* 290:140–145.

3. Smyth MJ, et al. (2004) NKG2D recognition and perforin effector function mediate effective cytokine immunotherapy of cancer. *J Exp Med* 200:1325–1335.
4. Remels L, Franssen L, Huygen K, De Baetselier P (1990) Poly I:C activated macrophages are tumoricidal for TNF- α -resistant 3LL tumor cells. *J Immunol* 144:4477–4486.

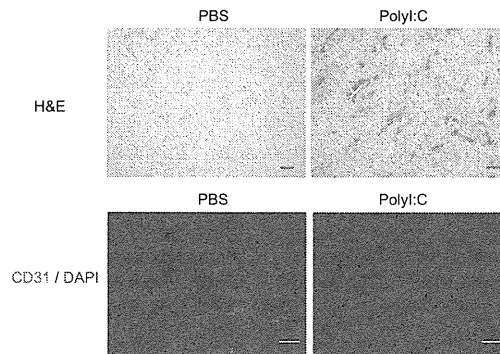


Fig. S1. PolyI:C induces hemorrhagic necrosis of tumor. 3LL tumor-bearing mice were i.p. injected with 200 μ g polyI:C and tumors were isolated 12 h later. Formalin-fixed tumors stained with H&E (*Upper*) and frozen sections stained with anti-CD31 antibody and DAPI nuclear stain (*Lower*). Original magnification 10 \times for all panels. (Scale bars, 100 μ m.) A representative experiment of three with similar outcomes is shown.

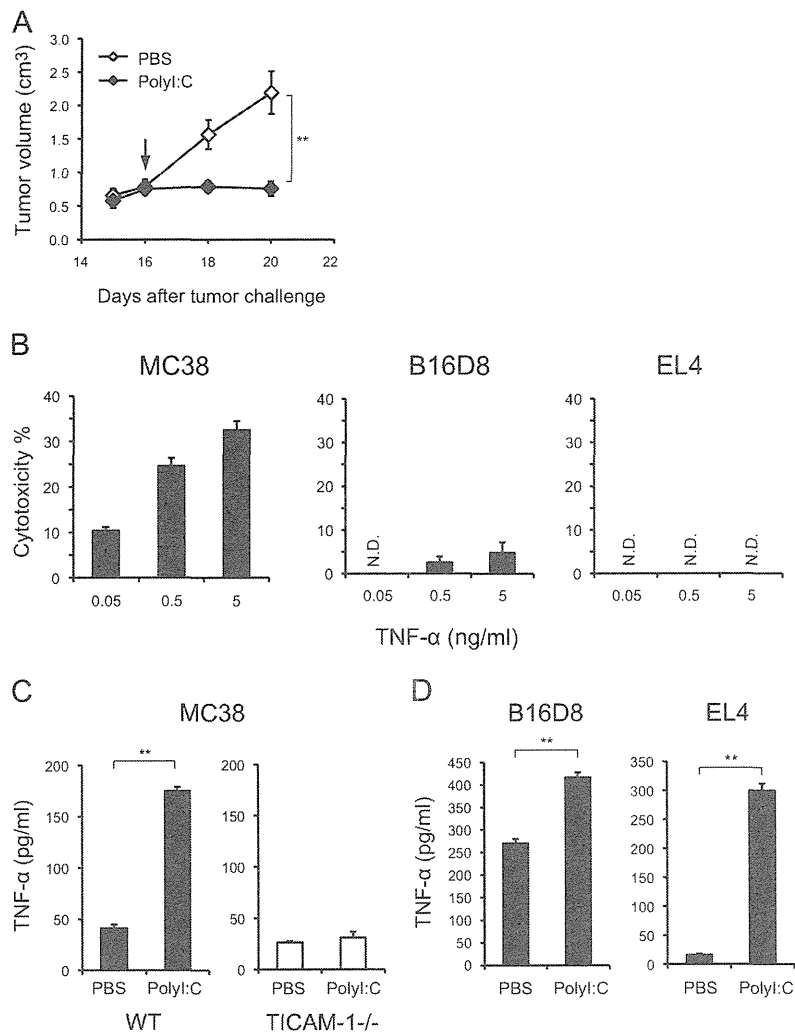


Fig. S2. PolyI:C induces TNF- α production by tumor-associated F4/80⁺ Mfs in various types of tumor. (A) MC38 cells (1×10^5) were s.c implanted into C57BL/6 mice (day 0). PolyI:C (200 μ g) was i.p. injected on day 16. Data are shown as tumor average size \pm SE; $n = 3-4$ mice per group. (B) Sensitivity of MC38, B16D8, and EL4 cells to recombinant TNF- α . (C and D) MC38, B16D8, and EL4 tumor-bearing mice were i.p injected with 200 μ g polyI:C. After 1 h, F4/80⁺ cells were isolated from tumors and incubated for 24 h. TNF- α concentration in the conditioned medium was determined by ELISA; $n = 3$. Data are shown as average \pm SD. N.D., not detected. A representative experiment of two with similar outcomes is shown.

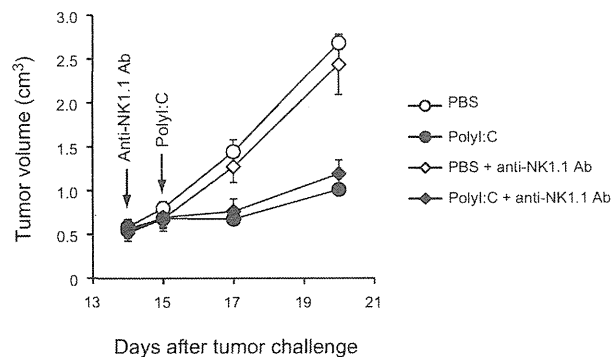


Fig. S3. NK cells are not essential for polyI:C-induced antitumor activity in vivo. 3LL tumor cells (3×10^6) were s.c transplanted into C57BL/6 mice (day 0). NK cells were depleted by injection of anti-NK1.1 antibody (PK136) into 3LL tumor-bearing mice on day 14. All doses of antibody and treatment regimens were determined in preliminary studies using the same lot of antibodies used for the experiments. Treatment was confirmed to deplete completely the desired cell populations for the entire duration of the study. PolyI:C (250 μ g) was i.p injected on day 15 and the tumor volume was measured. Data shown are means \pm SE, $n = 3$. A representative experiment of two with similar outcomes is shown.

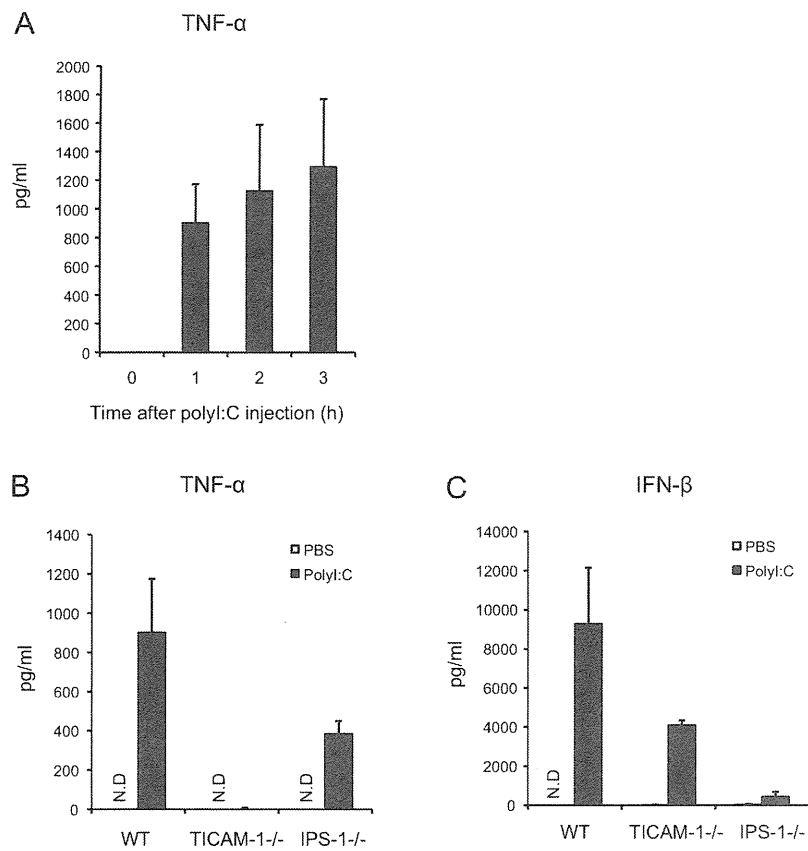


Fig. S4. Cytokine production in poly:I:C-treated mouse. (A) WT mice were injected i.p. with 200 μ g poly:I:C. After 0, 1, 2, and 3 h, TNF- α concentration in serum was determined by ELISA. (B and C) WT, TICAM-1^{-/-}, and IPS-1^{-/-} mice were injected i.p. with 200 μ g poly:I:C. After 1 h for TNF- α (B) and 4 h for IFN- β (C), serum cytokine levels were determined by ELISA. Data represents mean \pm SD ($n = 3$). N.D., not detected. A representative experiment of three with similar outcomes is shown.

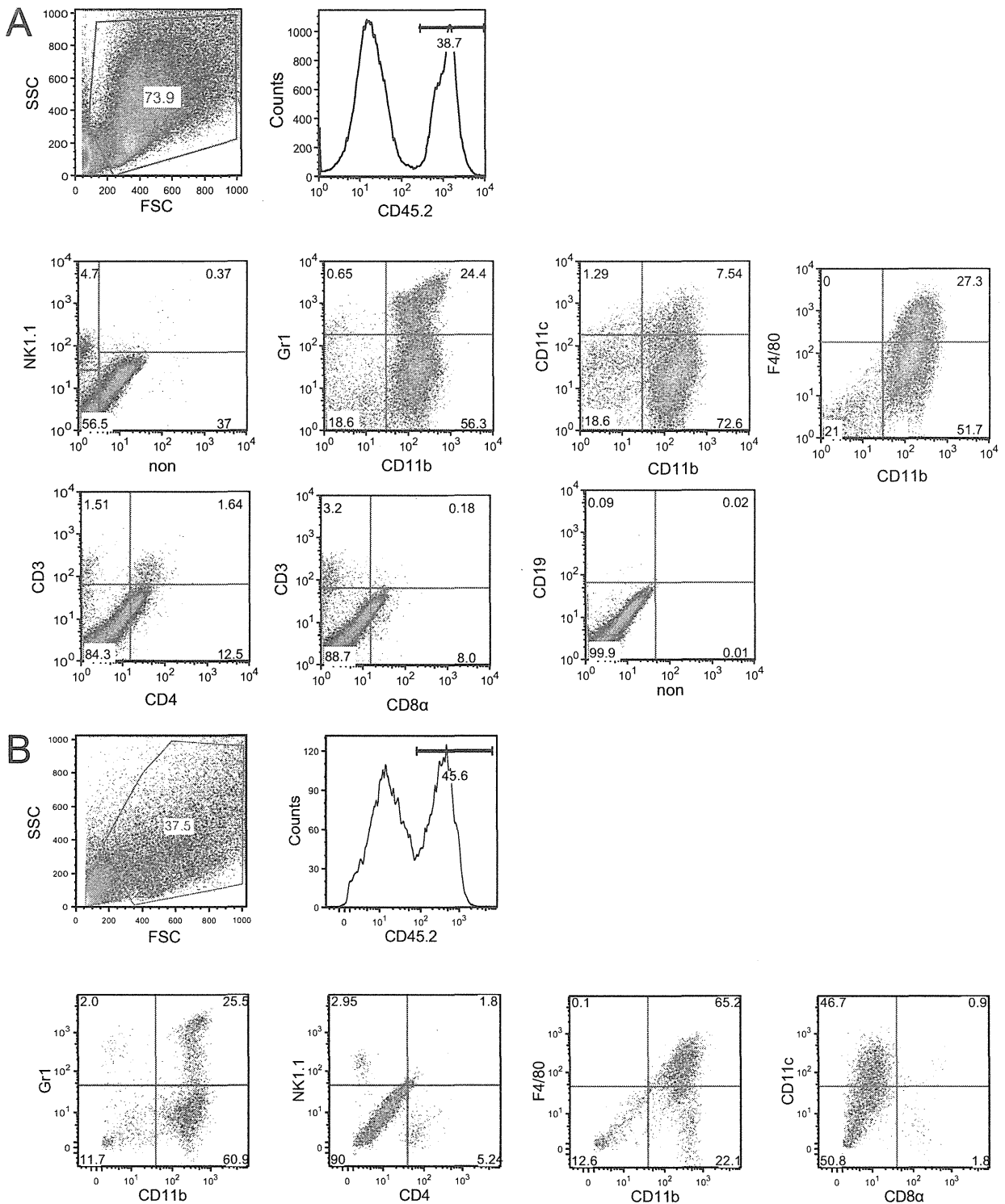
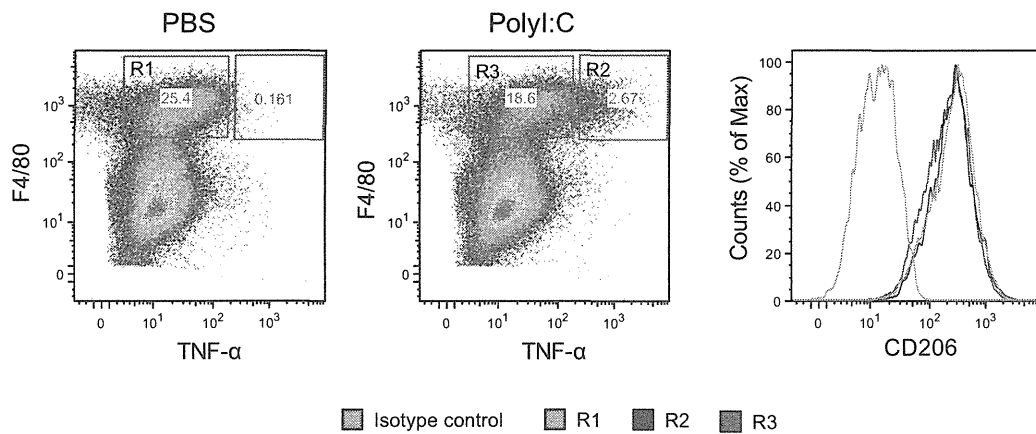


Fig. 55. Analysis of immune cells infiltrated into tumor. 3LL tumor cells (3×10^6) (A) or MC38 (1×10^6) (B) were transplanted s.c into B6 WT mice. After 2 wk, flow cytometric analysis was performed using freshly isolated whole tumor cell preparations in combination with staining of surface markers. CD45.2⁺ cells were gated, and the expression of indicated surface markers was further analyzed. Numbers represent percentage of the gated and positive cells. A representative experiment of two with similar outcomes is shown. FSC, forward scatter; SSC, side scatter.

A 3LL tumor



B Spleen (naive mouse)

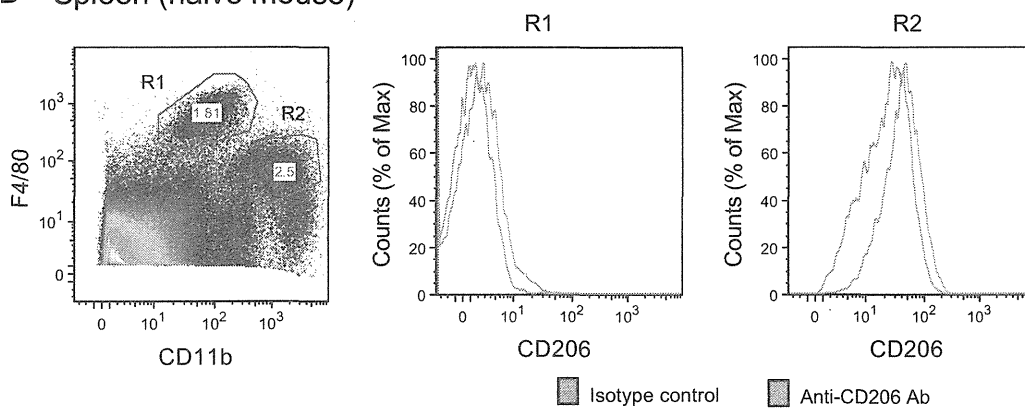


Fig. S6. Both TNF- α -producing and -nonproducing F4/80⁺ macrophages in 3LL tumor of polyI:C-injected mouse express CD206 (macrophage mannose receptor). (A) 3LL tumor-bearing mice were injected i.p with 200 μ g polyI:C. After 1 h, single-cell suspension of tumor was incubated in the presence of 10 μ g/mL Brefeldin A for 3 h. Intracellular cytokine staining for TNF- α in CD45.2⁺F4/80⁺ cells was performed. R2, and R1 and R3 indicates TNF- α -producing and -nonproducing F4/80⁺ cells, respectively. (B) CD206 expression in splenic F4/80⁺CD11b⁺ cells (R1 and R2) of naive mouse.

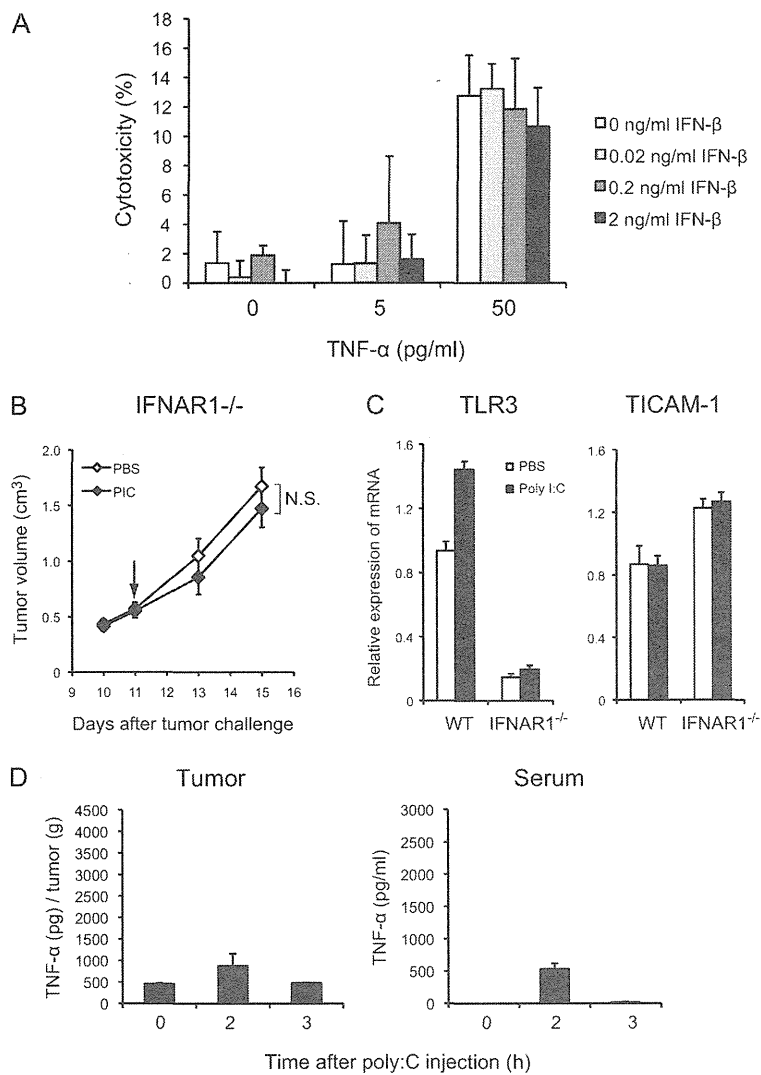


Fig. S7. Involvement of type I IFN signaling in 3LL tumor regression induced by poly:I:C. (A) Effect of IFN- β on cytotoxic activity of TNF- α against 3LL tumor cells. 3LL cells were incubated in the presence of 0, 5, and 50 pg/mL recombinant mouse TNF- α in combination with 0, 0.02, 0.2, and 2 ng/mL recombinant mouse IFN- β . Cytotoxicity was determined by ^{51}Cr release assay. (B) Disabling poly:I:C for 3LL tumor regression in IFN- α/β receptor (IFNAR1) $^{-/-}$ mice. Poly:I:C was i.p. injected on day 11; $n = 3\text{--}4$ mice per group. Data are shown as average \pm SE. N.S., not significant. (C) Levels of the mRNA of TLR3 and TICAM-1 in 3LL tumor-associated F4/80 $^{+}$ cells of WT or IFNAR1 $^{-/-}$ mice. (D) TNF- α levels in tumor and serum in poly:I:C-stimulated IFNAR1 $^{-/-}$ mice. Mice bearing 3LL tumors were i.p. injected with 200 μg poly:I:C. Tumor (Left) and serum (Right) were collected at 0, 2, and 3 h after poly:I:C injection, and TNF- α concentration was determined by ELISA. TNF- α level in tumor is presented as [TNF- α protein (pg)/tumor weight (g)].

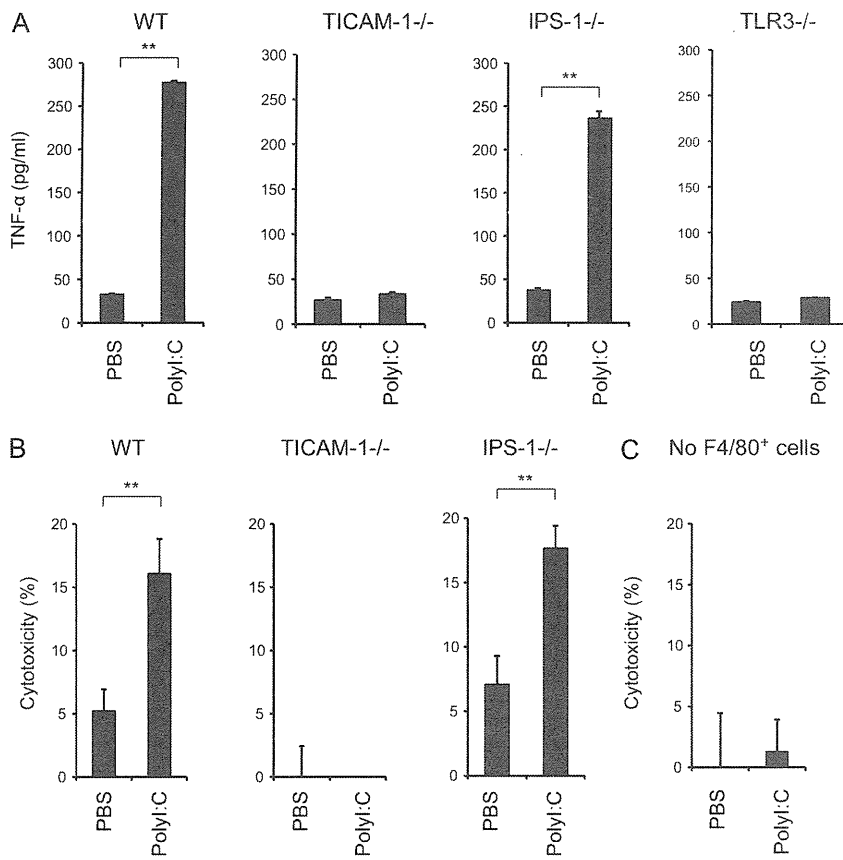


Fig. 58. In vitro polyI:C-stimulated F4/80⁺ cells secrete TNF- α and have cytotoxic activity. (A) F4/80⁺ cells isolated from 3LL tumor were stimulated with polyI:C (50 μ g/mL) in vitro. After 24 h, the conditioned medium was collected and TNF- α concentration was determined by ELISA. (B) F4/80⁺ cells isolated from tumor were mixed with ⁵¹Cr-labeled 3LL tumor cells in the presence or absence of polyI:C (50 μ g/mL). After 20 h, radioactivity of the conditioned medium was measured. E/T = 10. (C) ⁵¹Cr-labeled 3LL tumor cells were incubated for 20 h in the presence or absence of polyI:C (50 μ g/mL); $n = 3$. Data are shown as average \pm SD. ** $P < 0.001$. A representative experiment of three with similar outcomes is shown.

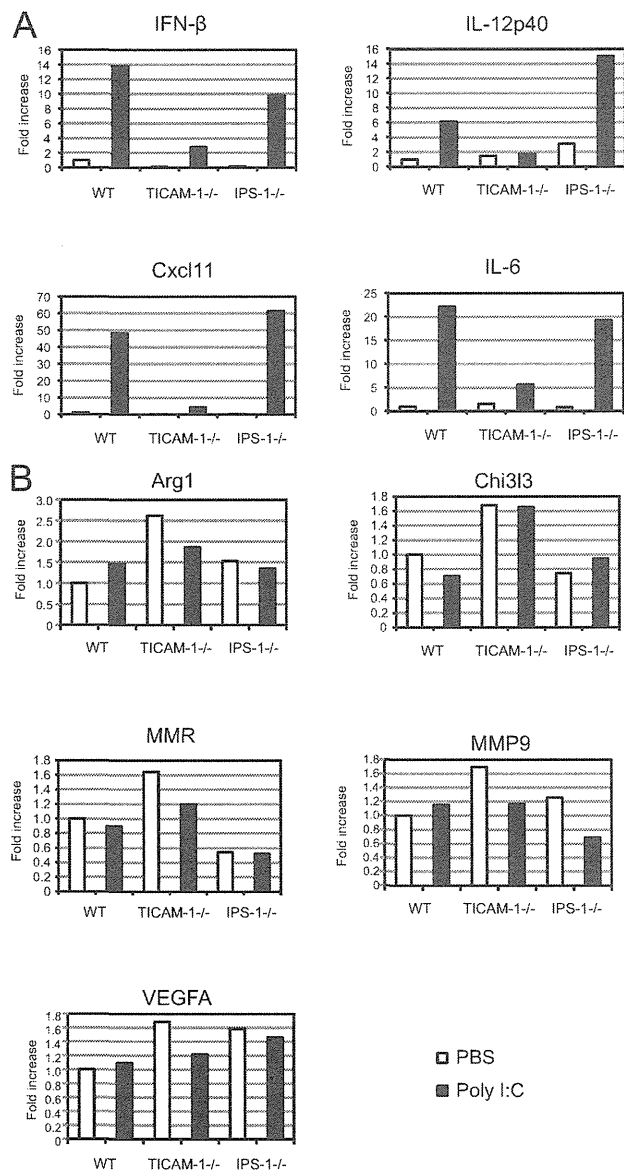


Fig. S9. PolyI:C induces the expression of M1 but not M2 macrophage-associated genes in tumor-infiltrated F4/80⁺ cells through the TICAM-1 pathway. 3LL tumor-bearing mice were i.p injected with 200 μ g polyI:C. After 3 h, tumors pooled from two mice treated with polyI:C or PBS were mixed. F4/80⁺ cells were isolated from the mixed tumor, and the expression of (A) M1- and (B) M2-related genes was analyzed. A representative experiment of two with similar outcomes is shown.